

NACA RM L53E21

7433

**NACA**

0144381

TECH LIBRARY KAFB, NM

RESEARCH MEMORANDUM

ENGINEERING METHOD OF RAM-JET THRUST DETERMINATION BASED
ON EXPERIMENTALLY OBTAINED COMBUSTOR PARAMETERS

By H. Rudolph Dettwyler and Maxime A. Faget

Langley Aeronautical Laboratory
Langley Field, Va.



**NATIONAL ADVISORY COMMITTEE
FOR AERONAUTICS**

WASHINGTON
August 13, 1953

**RECEIPT SIGNATURE
REQUIRED**





NATIONAL ADVISORY COMMITTEE FOR AERONAUTICS

RESEARCH MEMORANDUM

ENGINEERING METHOD OF RAM-JET THRUST DETERMINATION BASED
ON EXPERIMENTALLY OBTAINED COMBUSTOR PARAMETERS

By H. Rudolph Dettwyler and Maxime A. Faget

SUMMARY

A parameter is introduced which simplifies the accounting for pressure losses in ram-jet combustors. This parameter, called the combustor-force coefficient, relates the jet force and the total pressure at the combustion-chamber entrance. Experimental data for several different combustors are presented for evaluation and comparison. A calculation method is presented which reduces the ram-jet thrust equation to linear relationships and leads to a short method for determination of proper ram-jet free-stream tube area for a particular combustor considered.

INTRODUCTION

In connection with conducting free-flight performance investigations of ram-jet engines, the Langley Aeronautical Laboratory has continually been engaged in performance analysis of ram jets. Test data obtained from flight and preflight tests for ram jets burning vapor, liquid, and solid fuels have been analyzed. Various methods have been used to determine the level of performance of the ram-jet combustors. Early methods involved calculations that were long and tedious for the data-reduction process, as well as for the analysis process that uses the resulting parameters for determining performance at extrapolated conditions or for making new ram-jet designs.

It has been customary for some time to use air specific impulse as the parameter to express the heat-release rate in the combustor. The use of this parameter replaced the use of combustion flame temperature which was awkward and difficult to measure.

Another combustor performance parameter is presented herein. This parameter, called the "combustor-force coefficient," is developed through the use of one-dimensional analysis of the general energy, continuity,

~~CONFIDENTIAL~~

14-00000-92

and momentum equations to express the combustor jet force as a linear relationship with internal total pressure. The use of this parameter, which is easily measured, eliminates the separate determination of combustor friction losses, momentum losses due to heat addition, and the aerodynamic losses in the combustor exit nozzle. In addition, the use of the combustor-force coefficient, which is independent of all combustor environmental variables except entrance Mach number, greatly reduces the labor involved in making ram-jet performance calculations.

As a means for evaluation and comparison of this new parameter, experimental combustor-force coefficients for seven different units tested in several facilities are presented. A sample problem utilizing graphical solutions is presented to show how the analytical expression developed in this paper can be utilized.

The combustor-force coefficient simplifies the use of experimental data in solving for ram-jet thrust and internal pressures at conditions other than those at which tests were performed. The combustor-force coefficient, maximum total-pressure ratio, and maximum air specific impulse determine the optimum stream-tube area of entering air for maximum thrust coefficient. A simple equation is presented which relates these parameters for a quick solution to the matching problem.

SYMBOLS

A	area, sq ft
C_C	combustor-force coefficient, $G/H_1 A_1$
C_T	ram-jet thrust coefficient, $F/q_0 A_1$
F	ram-jet thrust, $G - \gamma_0 P_0 M_0^2 A_0 - P_0 A_4$, lb
f/a	fuel-air ratio
$f(M) = \frac{\left(1 + \frac{\gamma - 1}{2} M^2\right)^{\frac{\gamma}{\gamma - 1}}}{1 + \gamma M^2}$	
G	exit jet force, $PA(1 + \gamma M^2)$, lb
G^*	jet force (sonic exit), lb

g	gravitational acceleration, ft/sec ²
H	total pressure, lb/sq ft
H_0/P_0	isentropic pressure ratio, free stream
H_1/H_0	diffuser recovery
K	stagnation pressure ratio due to losses, H_{1a}/H_1
k	friction pressure-loss coefficient, $H_1 - H_{1a}/q_1$
M	Mach number
P	static pressure, lb/sq ft
q	dynamic pressure, lb/sq ft
R	universal gas constant, $\frac{1544}{\text{gas molecular weight}}$
S_a	exit air specific impulse, sec
S_a^*	air specific impulse (sonic exit), sec
T	static temperature, °F abs
T_S	stagnation temperature, °F abs
V	velocity, ft/sec
W_a	air mass flow, lb/sec
W_f	fuel mass flow, lb/sec
γ	ratio of specific heats
η_i	impulse efficiency, $S_{a\text{ act}}^*/S_{a\text{ theo}}^*$
ρ	specific mass density, slugs/ft ³
$\phi(M)$	nozzle expansion correction factor (ideal)

Subscripts:

0 free stream

1	diffuser exit
1a	imaginary station at combustor entrance at which all drag losses in the combustor have been considered to have occurred
2	combustion-chamber exit
3	nozzle throat
4	nozzle exit
act	actual
theo	theoretical

DETERMINATION AND USE OF COMBUSTOR-FORCE COEFFICIENT C_C

The thrust of a ram-jet engine is a result of the momentum and pressure forces acting on the stream tubes of gases entering and leaving the engine. Thus, with the use of the station subscripts defined in figure 1,

$$F = \rho_4 A_4 V_4^2 - \rho_0 A_0 V_0^2 + A_4 (P_4 - P_0) \quad (1)$$

This equation may be rewritten in Mach number terminology and reduced to

$$F = P_4 A_4 (1 + \gamma_4 M_4^2) - A_4 P_0 - \gamma_0 P_0 M_0^2 A_0 \quad (2)$$

The greatest difficulty in solving for values of ram-jet thrust lies in an accurate determination of the quantities appearing in the first term of the equation. This term is defined as the jet force G . Thus,

$$G = P_4 A_4 (1 + \gamma_4 M_4^2) \quad (3)$$

and, therefore,

$$F = G - A_4 P_0 - \gamma_0 P_0 M_0^2 A_0 \quad (4)$$

If the air specific impulse and weight flow of air are known, the jet force may be easily determined, since by definition

$$S_a = \frac{G}{W_a} \quad (5)$$

A value for air specific impulse may be obtained from

$$S_a = S_a^* \text{theo} \eta_1 \phi(M) \quad (6)$$

where $S_a^* \text{theo}$ is the theoretical value of the air specific impulse in a choking exit for the particular fuel-air ratio used, η_1 is the impulse efficiency, and $\phi(M)$ is the correction for increased thrust obtained by nozzle expansion. Expressions for $S_a^* \text{theo}$ and $\phi(M)$ are presented in appendix A. Values of η_1 may be obtained from experimental results, or may be based on past experiences with similar combustors. The use of values of air specific impulse in performance computations was explained in 1947 (ref. 1) and has been generally adopted as an engineering method of evaluating the thrust-producing potential of various fuels burned in air. It is therefore considered that no further explanation of this parameter is required.

The jet thrust G of a ram jet at any given free-stream condition may be limited by either the amount of heat being added to the entering air or by the pressure available at the exit nozzle. With a fixed mass flow and a choking condition the jet thrust of a given nozzle may be increased by increasing the total temperature and pressure of the gases. Under these conditions an increase in temperature will be accompanied by an increase in pressure and vice versa. While S_a allows the thrust to be determined on the basis of the mass flow of air entering the ram jet and the impulse available per pound of air after combustion, no consideration is given to the pressure losses throughout the engine and total pressure available from the free-stream conditions.

When the diffuser total-pressure recovery, the free-stream total pressure, and the combustor-force coefficient are known, the jet force may be determined as follows:

$$G = C_G H_1 A_1 \quad (7)$$

A value for C_G may be determined from experimental results or may be based on past experiences with similar combustors.

Appendix B presents a detailed discussion of the combustor-force coefficient and a method for determining values for this coefficient when values of the combustor pressure losses (in terms of the entrance dynamic pressure) are known. These losses are a result of friction and separation losses of the flame holder, shell, and nozzle and are the actual "hot" losses and not those associated with "cold" conditions.

The use of the combustor-force coefficient allows one to weigh directly the differences between any one combustor and nozzle combination and any others with respect to thrust potential based on pressure available at the combustor entrance. The analysis presented in appendix B shows that with a choking exit the combustor-force coefficient is independent of environmental conditions at any specified combustor entrance Mach number. The combustor-force coefficient for a combustor with an exit nozzle with a contraction and expansion ratio of 1.17 and various hypothetical internal-drag values from $1q$ to $6q$ is shown in figure 2. (The notation for internal drag is explained as follows: The pressure-loss coefficient k represents the stagnation-pressure drop referenced to the dynamic pressure, such as $k = \frac{H_1 - H_{1a}}{q}$. The internal-drag values kq , then, which are equivalent to the stagnation-pressure drop, are represented numerically herein in terms of the dynamic pressure, such as $1q$, $2q$, and so forth.) It is apparent that the lowest drag configuration will produce the highest combustor-force coefficient for a specified entrance Mach number. The variations of M_1 , when free-stream conditions are fixed, is synonymous to a fuel-air-ratio change. The real significance of the combustor-force coefficient is that it directly rates any one combustor with another, the highest value naturally being for the unit that can produce more thrust when considered in a ram jet of equal diffuser recovery and unit size. For example, consider the use of a combustor with a diffuser that delivers 10,000 pounds per square foot of total pressure for $M_1 = 0.20$ at specified flight conditions. In this case, the $1q$ combustor shown in figure 2 would produce a jet force of 9510 pounds for every square foot of combustion-chamber area, whereas the $6q$ unit would deliver only 8320 pounds of jet force per square foot.

In order to realize the higher jet force in the cited example, however, a correspondingly higher value of air specific impulse would be required. Under these conditions, when the diffuser recovery is not necessarily the maximum available, the maximum air specific impulse will dictate the maximum jet thrust.

In figure 3 the effect of varying the geometry of the exit nozzle is illustrated for a $4q$ combustor. Exit nozzles having the largest contraction ratio, and therefore the smallest throats, produce the lowest values of C_G . The use of a small throat may be desirable where

fuel economy becomes a major factor. In such a case, the throat size would be determined by the expansion ratio required to keep nozzle losses to a minimum.

The effect of a nonexpanding exit (sonic flow at the exit) would show the same general trends as in figures 2 and 3, but with lower values of C_G throughout. This is as should be expected, since an increase in momentum will result when the exit flow is expanded to a lower pressure. This gain in jet force is expressed as a nozzle factor which is described in appendix A.

CORRELATION OF COMBUSTOR DATA

An engineering analysis is valuable only when good agreement can be obtained with experimental data. Values of the combustor-force coefficient are presented for seven different combustors. These include combustors that use flame holders of three different types - gutter type, "donut" type, and can type. Sketches of the various combustor configurations are presented in figure 4. Some general information on these configurations is presented in table I. Connected duct, free-jet, and free-flight ram-jet data for the different combustor configurations are presented in figures 5 to 11. In these data the jet force was either a direct measurement or was computed from force measurements with the proper tare conditions considered. Combustor internal pressures were measured values from which Mach number and mass-flow conditions were determined. The jet force so obtained was divided by the product of the total pressure at combustor entrance and the combustor cross-sectional area, giving values of the combustor-force coefficient, C_G . These values of C_G were plotted against the combustor entrance Mach number M_1 .

In order to classify the combustors for each case, computed curves of C_G at constant drag conditions for each particular combustor geometry are superimposed on the test data. Therefore, by merely examining the curves, it can be seen that the test data will actually classify the combustor as to its apparent drag characteristics; that is, $2q$ or $4q$, and so forth. In considering figure 5 (combustor A), the test points fall on the $4q$ drag curve over the range of inlet Mach numbers tested, while the combustor-force coefficient varied from 0.80 to 0.73. These data are for free-jet Mach numbers of 1.84, 1.90, and 2.06 and a range of T_{S_0} from 830° F to 960° F absolute and a range of f/a from 0.009 to 0.078. Similar comparisons are made with the other combustor data presented.

The data for a 9.6-inch-diameter combustor with a modified donut burner (combustor B) are presented in figure 6. This burner was of a

~~CONFIDENTIAL~~

similar type used in combustor A, except that two concentric rows of donut flame holders were employed having approximately equal total geometric blocked area as combustor A. Vapor ethylene fuel was used and injected at the first flameholder. A nonexpanding exit nozzle with a contraction ratio of 1.25 was used. It should be noted that neither effects of free-jet Mach number nor stagnation temperature are evident. It is of interest to note that, although combustors A and B are not identical, figures 5 and 6 indicate that their drag and C_D conditions are equal.

Figure 7 presents data for a donut burner in a 6.5-inch-diameter unit (combustor C) with two different nozzles. This particular burner had the same percentage of internal blocked area and also employed the same combustor-chamber length as combustors A and B but was evaluated with an expanding exit. It is of interest to note, however, that the apparent drag of combustor C is somewhat lower than combustors A or B. This might be attributed to the relatively longer length between the flame holder farthest downstream and the exit, resulting in the immersed flame holders being in a lower velocity region. These data are for free-jet Mach numbers of 1.84, 2.06, and 2.21 at sea-level conditions. Again, it can be noted that free-jet M_0 and T_{S_0} had no effect on the drag or combustor-force coefficient over the range of M_1 shown. Flight data for similar units reported in references 2 and 3 are also presented for comparison. These data represented free-stream Mach numbers from 1.9 to 3.1 and an altitude range from near sea level to 67,000 feet. Figure 7(b) also shows data for $M_0 = 2$ from reference 4.

Free-jet data on a 16-inch-diameter combustor reported in reference 5 are presented in figure 8 (combustor D). The burner was of the corrugated-gutter type with fuel injection 17 inches upstream of the flame holder. These data are represented for $M = 1.35$ and $M = 1.73$ with a 90-inch combustion-chamber length and a nonexpanding exit-nozzle of area ratio 1.35. The maximum value of C_D indicated is 0.70 with a combustor drag of 8q. This high drag loss is probably largely due to the plug-type nozzle and support strut assembly utilized on this configuration. Because of the high internal-drag conditions prevailing, the combustor-force coefficient decreases rapidly with increased entrance Mach number M_1 .

Figure 9 presents data for a can-type burner in a 16-inch-diameter combustor reported in references 6 and 7 (combustor E). These data represent two exit-nozzle configurations at both $M_0 = 1.8$ and $M_0 = 2.0$. The evaluation and drag classification of this combustor with a straight-pipe exit is presented in figure 9(a). The combustor-force coefficient with a convergent-divergent nozzle ($A_4/A_3 = 1.4$) is shown in figure 9(b). Again these data indicate that the free-stream Mach number is an independent parameter; however, some apparent change in drag loss is indicated

when a nozzle with a contraction ratio is employed. This fact is evident when figures 9(a) and 9(b) are compared. The constant-area nozzle shows an over-all drag between $1q$ and $2q$, while C_G varied considerably with M_1 . In the case where a nozzle with a contraction and expansion ratio of 1.4 was tested, C_G remained practically constant, whereas the drag varied from $2q$ to $3q$ at the highest fuel-air ratios.

Figure 10 presents data obtained in duct tests (ref. 8) and free-jet tests of two combustors utilizing magnesium—JP-3 slurry fuel (combustors F and G). The free-jet data are for $M = 2.06$. These particular burners (modified vane-gutter flame holder and can type) were incorporated in a combustor-shell configuration similar to that of combustor C (fig. 4) with two expanding exits ($A_4/A_3 = 1.17$ and $A_4/A_3 = 1.28$). For combustor F, reducing the exit merely reduced the C_G available, whereas the over-all drag condition remained nearly constant (approx. $2\frac{1}{2}q$ at high values of f/a or the lowest values of M_1). This effect was previously predicted analytically by figure 3. Again, it is evident from figure 10 that the combustor-force coefficient is practically a linear variation with internal Mach number M_1 .

Data for the can-type burner were available only over a small range of values of M_1 for A_4/A_3 of 1.28 (combustor G). It is interesting to note that this unit has nearly identical drag characteristics and combustor-force coefficients for the limited range of M_1 tested as combustor F. In addition, when compared to a similar type of burner (combustor E, fig. 9(b)), it can be noted that both combustors have about the same internal drag conditions $2\frac{1}{2}q$, at equivalent M_1 .

The experimental effects of combustor exit-nozzle size on jet force are shown in figure 11 for combustor A. Previously, figure 5 indicated that this combustor with $A_4/A_3 = 1.25$ could be classified as a $4q$ unit. The addition data in figure 11 indicate that an increase or decrease of approximately 9 percent in exit-nozzle area ratio (nonexpanding type) has a marked effect on the over-all drag characteristics of the combustor. The exit-nozzle area ratios of 1.15 and 1.37 indicate $4\frac{1}{2}q$ and $3\frac{1}{2}q$ combustors, respectively. The increase in C_G with increased nozzle-throat area was predicted by the previously presented analytical discussion; however, the difference expected was not so large because of the change in apparent drag with different exit-nozzle sizes.

Experimental data from tests on combustors of different sizes, fuel types, and flame-holder configurations all showed good correlation with this parameter. Test experience on these combustors indicate that hot tests at one Mach number and stagnation temperature is sufficient to evaluate the combustor-force coefficient on any unit. This eliminates

the necessity for extensive testing programs in order to determine performance over a wide range of conditions.

The experimental data presented show that the exit force varies almost linearly with combustor entrance pressure. Thus, a measurement of this pressure should be easy to use as a thrust meter. References 9 and 10 discuss schemes of ram-jet controls utilizing such an engine-pressure measurement.

USE OF C_C AND S_a

Since the combustor-force coefficient relates the jet force to the internal pressure and the air specific impulse S_a is a measure of the jet impulse available due to combustion, each parameter can be used independently in an expression for ram-jet thrust and thrust coefficient.

By considering the air-specific-impulse parameter, equation (5), and substituting into equation (4), an expression for the thrust is obtained.

$$F = S_a W_a - A_4 P_0 - \gamma_0 P_0 M_0^2 A_0 \quad (8)$$

By dividing both sides by $q_0 A_1$, an expression for the thrust coefficient may be obtained. After simplifying and reducing to Mach number terminology,

$$C_T = 2 \left[\frac{S_a A_0}{M_0 A_1} \sqrt{\frac{g}{\gamma_0 R_0 T_0}} - \frac{A_4}{A_1 \gamma_0 M_0^2} - \frac{A_0}{A_1} \right] \quad (9)$$

By substituting equation (7) into equation (4), another expression for the thrust is obtained which considers the combustor-force coefficient

$$F = C_C H_1 A_1 - A_4 P_0 - \gamma_0 P_0 M_0^2 A_0 \quad (10)$$

Changing this to an expression for thrust coefficient in terms of Mach number and compression ratio yields

$$C_T = 2 \left[\frac{\left(\frac{H_1}{P_0} \right) C_C - \frac{A_4}{A_1}}{\gamma_0 M_0^2} - \left(\frac{A_0}{A_1} \right) \right] \quad (11)$$

The equations may be used to compute thrust and thrust coefficients of ram jets from experimental or estimated values of C_C , H_1/P_0 , and S_a . In making a performance map of a ram jet (where the variation of thrust is determined over a range of Mach numbers for various values of S_a and diffuser recovery) equations (9) and (11) are ideally suited for rapid computation. Equations (8) and (10) are useful for obtaining values of S_a and C_C from experimental data.

It should be noted that the jet force G is dependent upon two sets of conditions as set forth in equations (5) and (7). Thus,

$$G = S_a W_a = C_C H_1 A_1$$

From this relationship it can be concluded that, for a given ram jet under specified conditions, the jet thrust will be limited by either the air specific impulse or total pressure at the combustor entrance. If the air specific impulse limits the jet thrust, the total pressure at the combustor entrance H_1 will automatically conform to satisfy the equation. Similarly, if the total-pressure recovery limits the jet thrust, then either S_a will be less than maximum or the diffuser will automatically spill enough air so that W_a will be reduced until the product $S_a W_a$ will equal the jet thrust produced.

In designing ram jets, proper selection of the ratio of free-stream tube area to combustor area is necessary in matching diffuser to combustor characteristics. At the design Mach number, the engine should be designed to operate at maximum total-pressure recovery and maximum heat release. In order to determine the proper area ratio for conditions of maximum recovery and maximum S_a , equations (5) and (7) are combined.

$$S_a W_a = C_C H_1 A_1 \quad (12)$$

or

$$S_a P_0 M_0 A_0 \sqrt{\frac{\gamma_0 g}{R_0 T_0}} = C_C H_1 A_1 \quad (13)$$

Thus,

$$\frac{A_0}{A_1} = \frac{H_1}{P_0} \frac{C_C \sqrt{\frac{R_0 T_0}{\gamma_0 g}}}{S_a M_0} \quad (14)$$

It has been shown that C_C usually varies slightly with combustor-entrance Mach number M_1 . Since M_1 varies with area ratio for a given pressure recovery, the area ratio may not be determined directly; however, since the change in C_C with M_1 is slight, A_0/A_1 can be determined in one or two reiterations. Examination of equation (14) shows that, in order to utilize an increase in total-pressure recovery or combustor-force coefficient, a corresponding increase in A_0 is required; whereas a decrease in A_0 will be required to accommodate an increase in S_a .

CONCLUDING REMARKS

A study of the experimental data presented indicates consistent agreement between the engineering method of combustor evaluation and classification and the experimental data. This comparison has been done by means of evaluating seven completely different and independent configurations. Inasmuch as the combustor-force coefficient relates the jet force to the internal total pressure, it rates the thrust potential of the combustor in terms of the available pressure. One-dimensional analysis presented indicates that, when choking exists at the exit, the combustor-force coefficient should be independent of environmental conditions except for second-order combustor-entrance Mach number effects.

Some definite trends that resulted from experimental data presented are the following:

1. The free-stream Mach number variation from 1.35 to 3.1 shows no effect on combustor-force coefficient.
2. Free-stream stagnation temperature variation from 500° F to 1200° F absolute showed no determinable effects on combustor-force coefficient.

~~CONFIDENTIAL~~

3. The variation of nozzle throat size had a direct effect on combustor-force coefficient. In addition, small changes in apparent drag loss were indicated as the nozzle size was changed.

4. For the experimental tests evaluated, combustor-force coefficient decreased as the combustor-entrance Mach number increased. In many cases, however, the variation of combustor-force coefficient with combustor-entrance Mach number was very slight.

Test experience on these combustors indicates that hot tests at one Mach number and stagnation temperature will evaluate any unit, eliminating the necessity for extensive testing programs. The good experimental correlation shown indicates that a thrust meter or controlling device based upon combustor-entrance pressure measurement would be a workable device.

The use of the combustor-force coefficient and the air specific impulse parameter leads to simple ram-jet thrust-coefficient relationships, which allows for quick solutions. The problem of ram-jet sizing is simplified by the use of an expression using the combustor-force coefficient and air specific impulse. This expression allows for quick solution of the proper ram-jet free-stream tube area A_0 for a particular combustor considered.

Langley Aeronautical Laboratory,
National Advisory Committee for Aeronautics,
Langley Field, Va., May 27, 1953.

~~CONFIDENTIAL~~

APPENDIX A

DERIVATION OF AIR SPECIFIC IMPULSE, S_a

By definition (ref. 1) the air specific impulse is defined as the ratio between the exit momentum or jet exit force G and the air mass flow W_a . Expressing S_a in terms of stagnation temperature and γ results in an equation that allows a theoretical calculation of S_a^* for any fuel burned in air when thermal choking takes place in the exit nozzle. The jet force is defined

$$G = \rho A V^2 + P A = \rho A V g \left(\frac{V}{g} + \frac{P}{\rho V g} \right) \quad (15)$$

or

$$G = (W_a + W_f) \frac{V + \frac{P}{\rho V}}{g} \quad (16)$$

The Mach number in the exit is sonic; thus, equation (16) can be rewritten

$$G^* = (W_a + W_f) \frac{\frac{\gamma g R T + g R T}{\sqrt{\gamma g R T}}}{g} \quad (17)$$

Since $S_a^* = \frac{G^*}{W_a}$,

$$S_a^* = \left(\frac{W_a + W_f}{W_a} \right) \frac{\sqrt{\gamma g R T} + \sqrt{\frac{g R T}{\gamma}}}{g} \quad (18)$$

Simplifying gives

$$S_a^* = \left(1 + \frac{f}{a}\right)(\gamma + 1) \sqrt{\frac{RT}{\gamma g}} \quad (19)$$

Since $T = \frac{2T_g}{\gamma - 1}$ (for $M = 1$),

$$S_a^* = \left(1 + \frac{f}{a}\right) \sqrt{\frac{2(\gamma + 1)RT_g}{\gamma g}} \quad (20)$$

Equation (20) shows that the theoretical S_a^* can be obtained for any combustible fuel-air mixture provided the ratio of specific heats, the gas constant, and the stagnation temperature are known for the products of combustion corresponding to a given fuel-air ratio.

Since S_a^* is a measure of the ram-jet exit impulse, the impulse efficiency can be simply expressed as

$$\eta_i = \frac{S_{a \text{ act}}^*}{S_{a \text{ theo}}^*} \quad (21)$$

at the equivalent values of f/a and T_g .

Generally, the ram-jet combustor employs an expanding exit nozzle. Therefore, an increase in thrust is realized due to expanding the flow to a lower pressure. In order to express the air specific impulse at the nozzle exit, a nozzle correction factor $\phi(M)$ is required. Thus, the exit S_a is

$$S_a = S_a^* \phi(M) \quad (22)$$

This nozzle factor can be determined from stations 3 to 4 by assuming γ constant and no losses or separation effects (ref. 11).

$$\phi(M) = \frac{1 + \gamma_3 M_4^2}{M_4 \left[2(1 + \gamma_3) \left(1 + \frac{\gamma_3 - 1}{2} M_4^2 \right) \right]^{1/2}} \quad (23)$$

Where M_4 is found from the continuity equation

$$\frac{A_4}{A_3} = \frac{1}{M_4} \left(\frac{1 + \frac{\gamma_3 - 1}{2} M_4^2}{1 + \frac{\gamma_3 - 1}{2}} \right)^{\frac{\gamma_3 + 1}{2(\gamma_3 - 1)}} \quad (24)$$

Figure 12 presents the variation of S_a^* against f/a for a typical hydrocarbon fuel burned in air at free-stream stagnation temperature from 700°F absolute to 1000°F absolute. The nozzle factor $\phi(M)$ is presented in figure 13 as a function of area ratio for $\gamma = 1.4$ and $\gamma = 1.3$.

APPENDIX B

ANALYTICAL DETERMINATION OF COMBUSTOR-FORCE COEFFICIENT, C_C

The analysis considers a combustor of constant cross-sectional area (fig. 1) with some form of an exit restriction. The term "combustor" is considered to consist of three components - burner, shell, and exit nozzle. The burner component is considered made up of the fuel-injection and flame-holder systems.

For the analysis of this constant-area combustor, choking is assumed to exist in the combustor exit nozzle. The combustor drag consists of the pressure losses due to friction and separation. It is assumed that all of the losses not associated with heat addition take place before the combustion process. No special account is taken of the effects of fuel injection on the mass flow and gas velocity through the combustion zone and the aerodynamic efficiency of the exit nozzle; however, these losses are included as pressure losses based on entrance dynamic pressures and are definitely evaluated when hot-test data are employed. The ratio of specific heats is considered equal to that for standard air up to the combustion zone. In the combustion zone, γ is considered equal to 1.30. If desired, other values of γ can be used for the combustion zone; however, when experimental values are compared to computed values where $\gamma = 1.3$ was assumed, good correlation exists. Combustors are classified as to their drag characteristics in terms of total-pressure losses referenced to the entrance dynamic pressure; that is, $2q$, $4q$, and so forth.

The analysis is made in two steps - an independent expression for friction losses and an expression for the change in momentum due to heat addition. In the first step, all of the pressure losses due to friction and separation are taken between stations 1 and 1a (fig. 1), with no change in mass considered. By assuming the condition

$$H_{1a} = (H_1 - kq_1) \quad (25)$$

where q_1 represents the dynamic pressure at station 1 and k is the pressure loss coefficient. An expression for the stagnation pressure ratio K as a function of Mach number and γ is developed.

$$K = \frac{H_{1a}}{H_1} = 1 - k \left[\left(\frac{\gamma_1}{2} \right) \frac{M_1^2}{\left(1 + \frac{\gamma_1 - 1}{2} M_1^2 \right)^{\frac{\gamma_1}{\gamma_1 - 1}}} \right] \quad (26)$$

~~CONFIDENTIAL~~

Equation (26) is presented graphically in figure 14 for different amounts of pressure loss expressed in q against combustion-chamber entrance Mach number M_1 .

The Mach number of the flow at the entrance to the combustion zone M_{1a} , however, differs from the Mach number at the inlet M_1 because of the pressure losses experienced by the flow. Once q_1 and K are known at a particular M_1 , the new Mach number M_{1a} is obtained by one-dimensional flow analysis. Figure 15 presents a graphical solution for the M_{1a} for a range of dynamic pressure drops.

In the second step of the analysis, a momentum balance between stations 1a and 2 for a constant-area channel can be written (friction already having been accounted for)

$$P_{1a} + \rho_{1a} V_{1a}^2 = P_2 + \rho_2 V_2^2 \quad (27)$$

Since

$$P + \rho V^2 = P(1 + \gamma M^2) \quad (28)$$

then

$$P_{1a}(1 + \gamma_{1a} M_{1a}^2) = P_2(1 + \gamma_2 M_2^2) \quad (29)$$

Thus,

$$\frac{P_{1a}}{P_2} = \frac{1 + \gamma_2 M_2^2}{1 + \gamma_{1a} M_{1a}^2} \quad (30)$$

The total-pressure ratio due to heat addition can be found by employing the following tautology

$$\frac{H_2}{H_{1a}} = \frac{\frac{H_2}{P_2}}{\frac{H_{1a}}{P_{1a}}} \frac{P_2}{P_{1a}} \quad (31)$$

CONFIDENTIAL

By substituting equation (30) and the relationship

$$\frac{H}{P} = \left(1 + \frac{\gamma - 1}{2} M^2\right)^{\frac{\gamma}{\gamma-1}} \quad (32)$$

into equation (31), the total pressure becomes

$$\frac{H_2}{H_{1a}} = \frac{\left(1 + \frac{\gamma_2 - 1}{2} M_2^2\right)^{\frac{\gamma_2}{\gamma_2-1}}}{\left(1 + \frac{\gamma_{1a} - 1}{2} M_{1a}^2\right)^{\frac{\gamma_{1a}}{\gamma_{1a}-1}}} \frac{\left(1 + \gamma_{1a} M_{1a}^2\right)^{\frac{\gamma_{1a}}{\gamma_{1a}-1}}}{\left(1 + \gamma_2 M_2^2\right)^{\frac{\gamma_2}{\gamma_2-1}}} \quad (33)$$

For purposes of simplicity, let

$$f(M) = \frac{\left(1 + \frac{\gamma - 1}{2} M^2\right)^{\frac{\gamma}{\gamma-1}}}{1 + \gamma M^2} \quad (34)$$

Then

$$\frac{H_2}{H_{1a}} = \frac{f(M_2)}{f(M_{1a})} \quad (35)$$

After considering other losses exclusive of those due to heat addition

$$\frac{H_2}{H_1} = K \frac{f(M_2)}{f(M_{1a})} \quad (36)$$

Equation (36) thus expresses the pressure ratio in a constant-area channel due to pressure and separation losses and the ideal heat-addition process in terms of Mach number.

For purposes of simplicity, it is assumed that no total-pressure losses occur through the exit nozzle; that is, $H_2 = H_4$. It should be noted that such losses that do occur are charged to combustor-friction losses. Considering the conditions at station 4, the jet force G can be written as

$$G = P_4 A_4 (1 + \gamma_4 M_4^2) \quad (37)$$

By solving equation (32) for P and substituting into equation (37), the jet force becomes

$$G = \frac{A_4 H_4 (1 + \gamma_4 M_4^2)}{\left(1 + \frac{\gamma_4 - 1}{2} M_4^2\right)^{\frac{\gamma_4}{\gamma_4 - 1}}} \quad (38)$$

Simplifying with equation (34)

$$G = \frac{A_4 H_4}{f(M_4)}$$

or, since $H_2 = H_4$

$$G = \frac{A_4 H_2}{f(M_4)} \quad (39)$$

By solving equation (36) for H_2 and substituting in equation (39), the jet force becomes

$$G = \frac{K H_1 A_4 f(M_2)}{f(M_{1a}) f(M_4)} \quad (40)$$

~~CONFIDENTIAL~~

By dividing G by the total pressure and area at station 1, a non-dimensional coefficient results which is called the combustor-force coefficient, C_C .

$$C_C = \frac{G}{H_1 A_1} = K \frac{A_4}{A_1} \frac{f(M_2)}{f(M_{1a})f(M_4)} \quad (41)$$

For most cases $A_4 = A_2 = A_1$ (as in fig. 1); thus, equation (41) may be written as

$$C_C = K \frac{f(M_2)}{f(M_{1a})f(M_4)} \quad (42)$$

Another special case to consider is that of a constant-area nozzle and combustor, $A_1 = A_2 = A_3 = A_4$. Under such conditions equation (41) simplifies to

$$C_C = \frac{K}{f(M_{1a})} \quad (43)$$

because $f(M_2)$ and $f(M_4)$ are equal.

As an aid for quick solutions to equations (41), (42), and (43), the functions K , A_2/A_3 , A_4/A_3 , $f(M)$ in the subsonic case, and $f(M)$ in the supersonic case are presented against Mach number in figures 14 to 17.

Example of the Use of Charts

The use of the appropriate functions presented in figures 14 to 17 to compute a combustor-force coefficient can be shown with the following sample problem:

Determine the combustor-force coefficient for a combustor with the following qualifications:

$$M_1 = 0.20$$

$$\gamma_2 = \gamma_3 = \gamma_4 = 1.3$$

$$\gamma_1 = \gamma_{1a} = 1.4$$

$$\frac{A_2}{A_3} = \frac{A_4}{A_3} = 1.20$$

4q burner

Solution:

Known quantities	Figure used	Find
$M_1 = 0.20$; drag loss = 4q ₁	14	$K = 0.881$
$M_1 = 0.20$; drag loss = 4q ₁	15	$M_{1a} = 0.233$
$A_2/A_3 = 1.2$; $\gamma_2 = 1.3$	16(a)	$M_2 = 0.593$
$A_4/A_3 = 1.2$; $\gamma_4 = 1.3$	16(b)	$M_4 = 1.515$
$M_{1a} = 0.233$; $\gamma_{1a} = 1.4$	17(a)	$f(M_{1a}) = 0.961$
$M_2 = 0.593$; $\gamma_2 = 1.3$	17(a)	$f(M_2) = 0.858$
$M_4 = 1.515$; $\gamma_4 = 1.3$	17(b)	$f(M_4) = 0.902$

Knowing K , $f(M_{1a})$, $f(M_2)$, and $f(M_4)$, use equation (42) to find the combustor-force coefficient

$$C_G = \frac{0.881 \times 0.858}{0.961 \times 0.902} = 0.872 \text{ (answer)}$$

~~CONFIDENTIAL~~

REFERENCES

1. Rudnick, Philip: Momentum Relations in Propulsive Ducts. Jour. Aero. Sci., vol. 14, no. 9, Sept. 1947, pp. 540-544.
2. Faget, Maxime A., and Dettwyler, H. Rudolph: Initial Flight Investigation of a Twin-Engine Supersonic Ram Jet. NACA RM L50H10, 1950.
3. Dettwyler, H. Rudolph, and Bond, Aleck C.: Flight Performance of a Twin-Engine Supersonic Ram Jet From 2,300 to 67,200 Feet Altitude. NACA RM L50L27, 1951.
4. Faget, Maxime A., Watson, Raymond S., and Bartlett, Walter A., Jr.: Free-Jet Tests of a 6.5-Inch-Diameter Ram-Jet Engine at Mach Numbers of 1.81 and 2.00. NACA RM L50L06, 1951.
5. Perchonok, Eugene, and Farley, John M.: Internal Flow and Burning Characteristics of 16-Inch Ram Jet Operating in a Free Jet at Mach Numbers of 1.35 and 1.73. NACA RM E51C16, 1951.
6. Nussdorfer, T. J., Wilcox, F., and Perchonok, E.: Investigation at Zero Angle of Attack of a 16-Inch Ram-Jet Engine in 8- by 6-Foot Supersonic Wind Tunnel. NACA RM E50L04, 1951.
7. Perchonok, Eugene, Wilcox, Fred A., and Pennington, Donald: Effect of Angle of Attack and Exit Nozzle Design on the Performance of a 16-Inch Ram Jet at Mach Numbers from 1.5 to 2.0. NACA RM E51G26, 1951.
8. Branstetter, J. Robert, Gibbs, James B., and Kaufman, Warner B.: Magnesium-Slurry Combustion Performance in a 6.5-Inch-Diameter Ram-Jet Engine Mounted in a Connected-Pipe Facility. NACA RM 1953.
9. Faget, Maxime A.: A Proposed Ram-Jet Control System Operated by Use of Diffuser Pressure Recovery. NACA RM L52E05b, 1952.
10. Himmel, Seymour C.: Some Control Considerations of Ram-Jet Engines. NACA RM E52F10, 1952.
11. Beer, A. C.: An Analytical Approach to Ramjet Design Optimization. Bumblebee Rep. No. 108, The Johns Hopkins Univ., Appl. Phys. Lab., Dec. 1949.

~~CONFIDENTIAL~~

TABLE I
COMBUSTOR AND BURNER DATA

No.	Type	Maximum blockage, percent	Maximum burner diameter, in.	Shell inside diameter, in.	Fuel	Reference
A	Donut	24.7	6.00	9.65	Ethylene	-----
B	Modified donut	25.6	7.00	9.65	Ethylene	-----
C	Donut	25.0	4.00	6.50	Ethylene	2, 3, 4
D	Corrugated gutter	54.0	16.00	16.0	Gasoline	5
E	Can	133.0 (open)	14.38	16.0	Propylene oxide	6, 7
F	Vane gutter	46.0	5.00	6.5	Magnesium slurry	8
G	Can	120.0 (open)	6.00	6.5	Magnesium slurry	-----


 NACA
~~CONFIDENTIAL~~

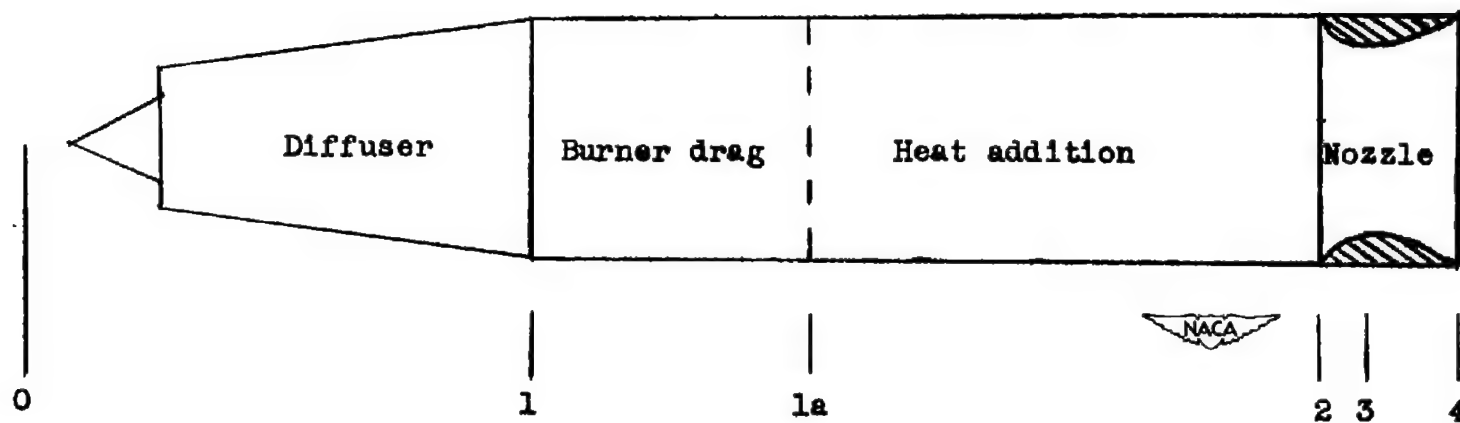


Figure 1.- Sketch of ram-jet configuration used in analysis.

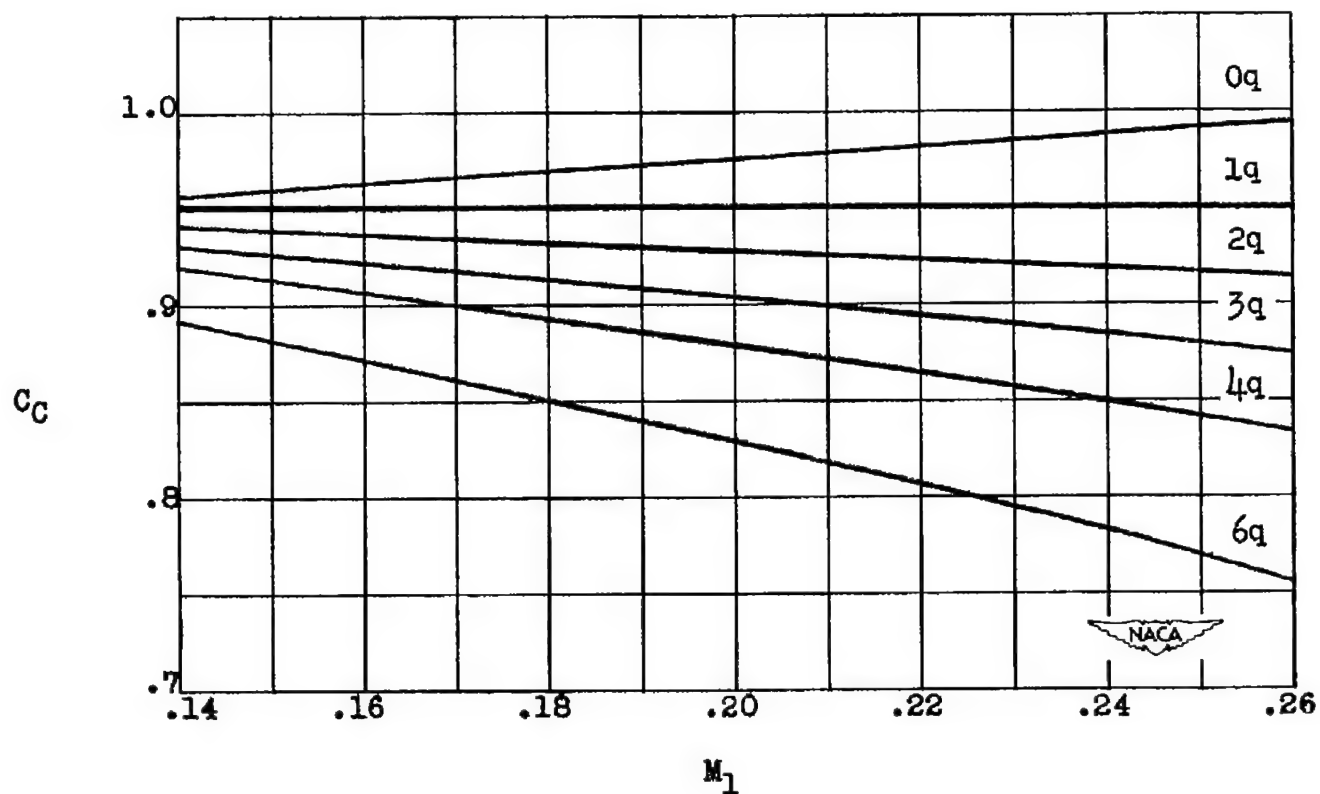


Figure 2.- Variation of combustor-force coefficient C_C with M_1 at different internal-drag conditions and an expanding exit nozzle, $A_4/A_3 = 1.17$.

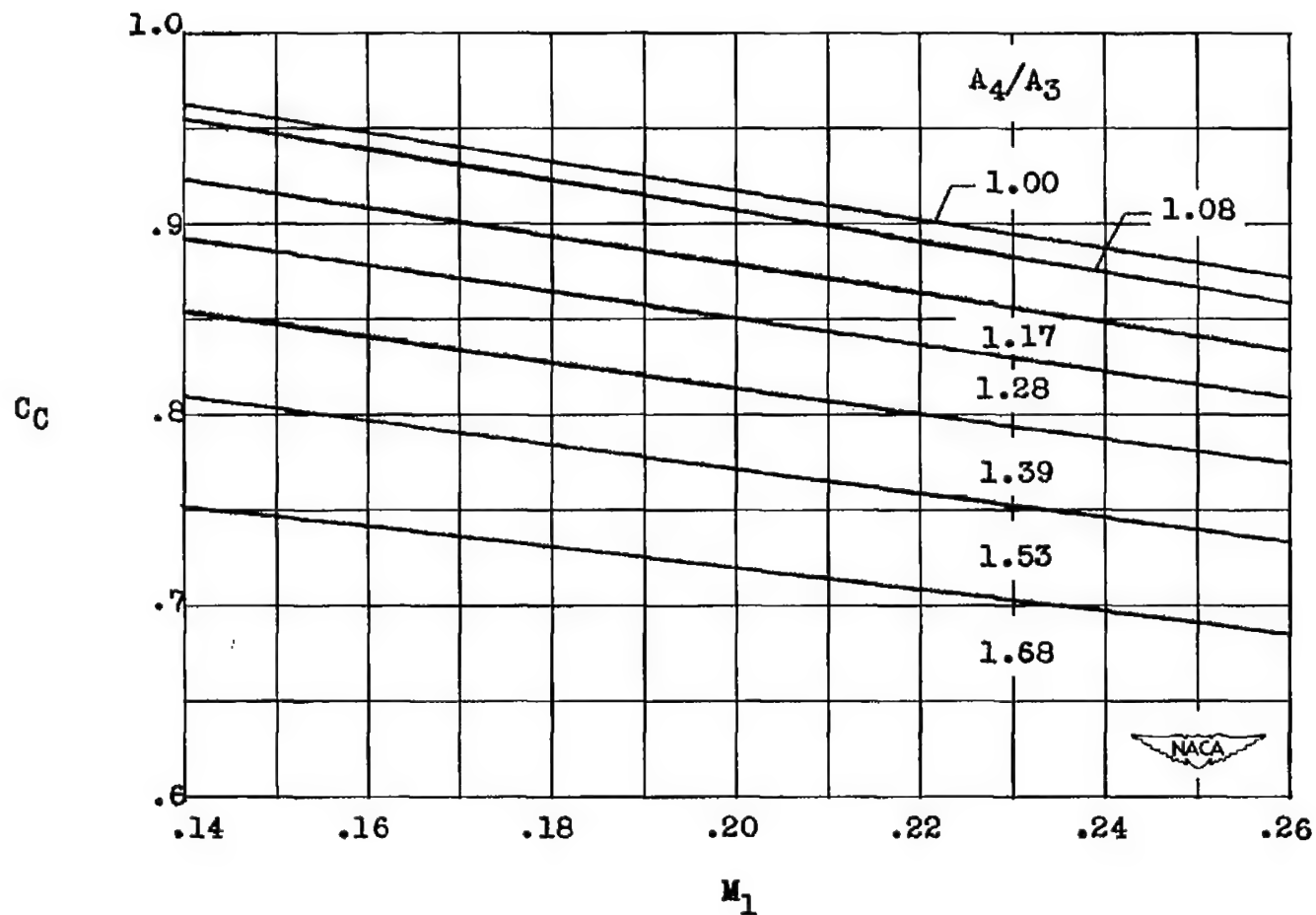
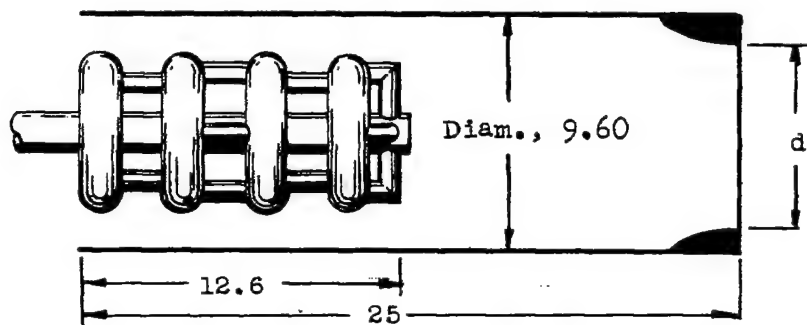
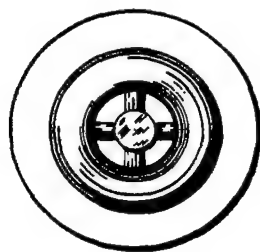
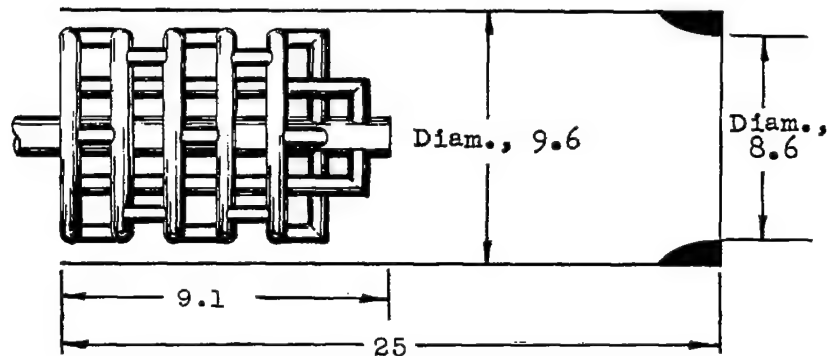
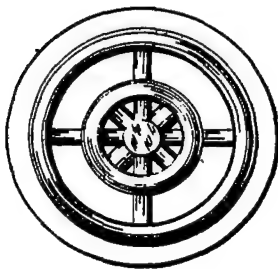


Figure 3.- The effect of expanding exit nozzle sizes on combustor-force coefficient C_c in a 4q combustor.

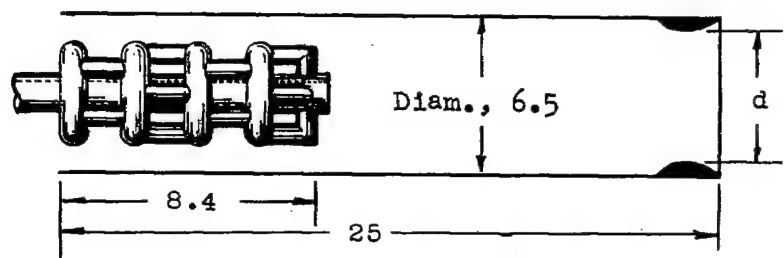
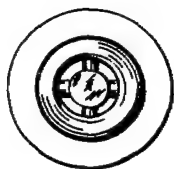


Combustor A

Diam., d
9.0
8.6
8.3



Combustor B

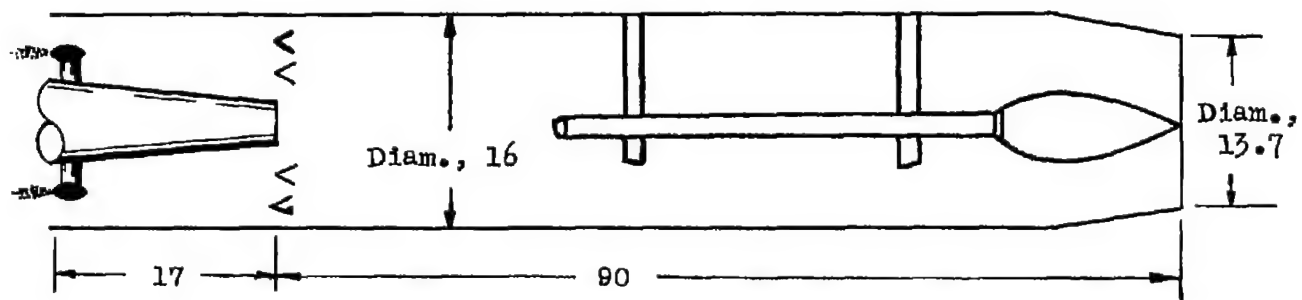
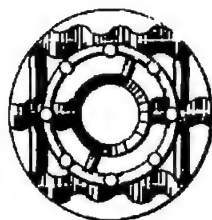


Combustor C

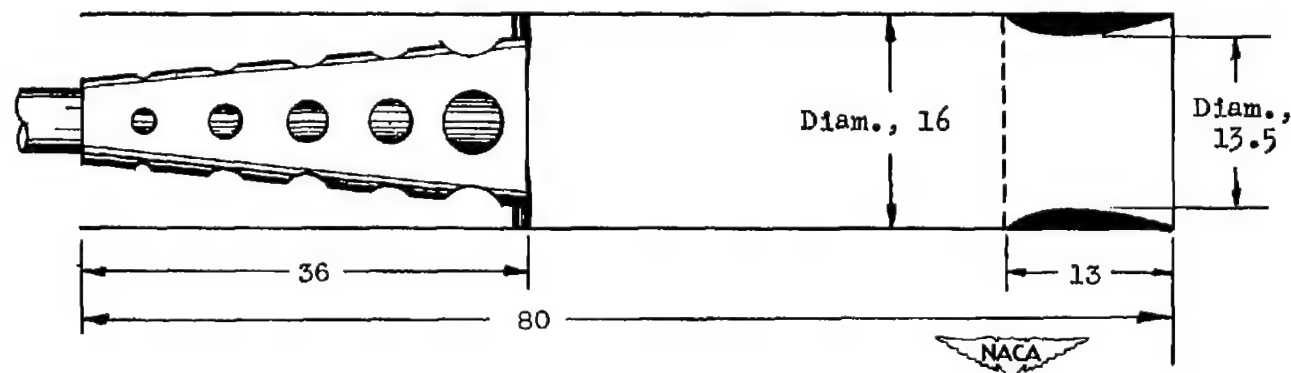
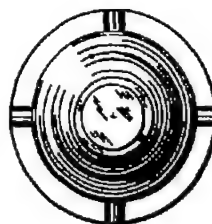


Diam., d
6.0
5.7

Figure 4.- Sketch of combustor configurations evaluated. All dimensions are in inches.

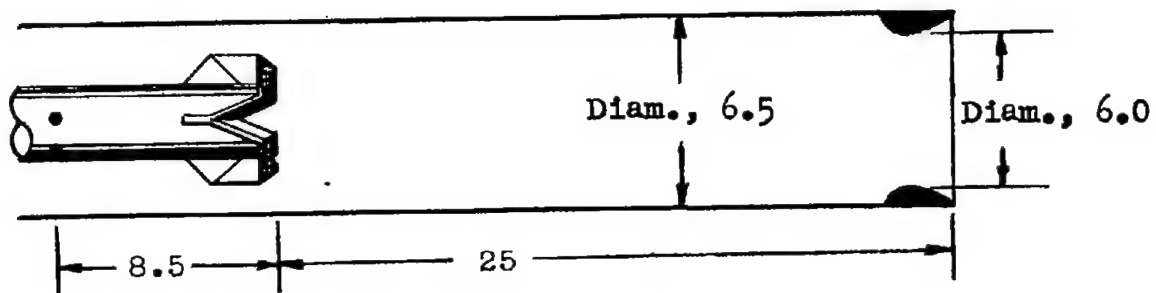
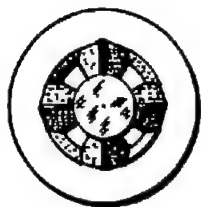


Combustor D

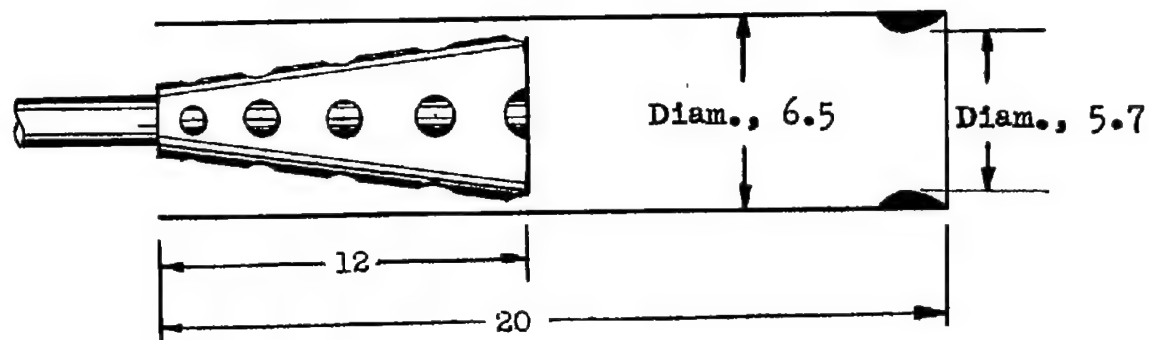
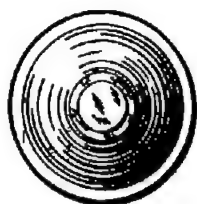


Combustor E

Figure 4.- Continued.



Combustor F



Combustor G

Figure 4.- Concluded.



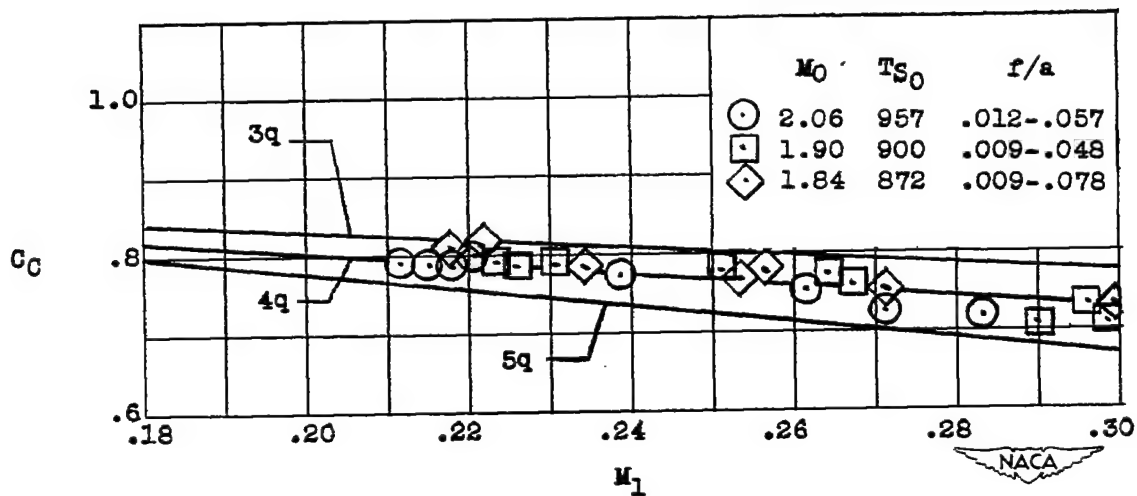


Figure 5.- Combustor A. Nonexpanding exit, $A_4/A_3 = 1.25$; multiflameholder.

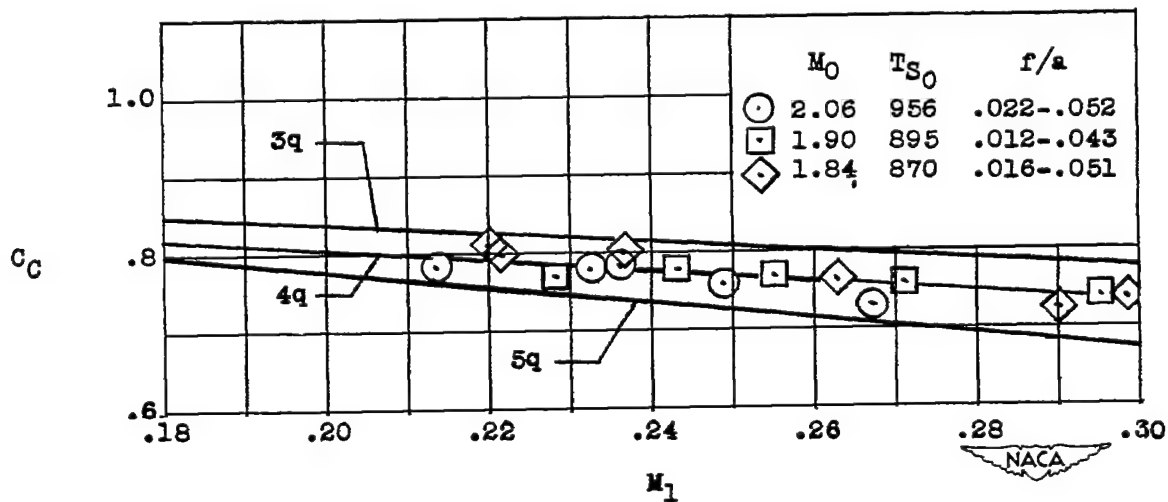
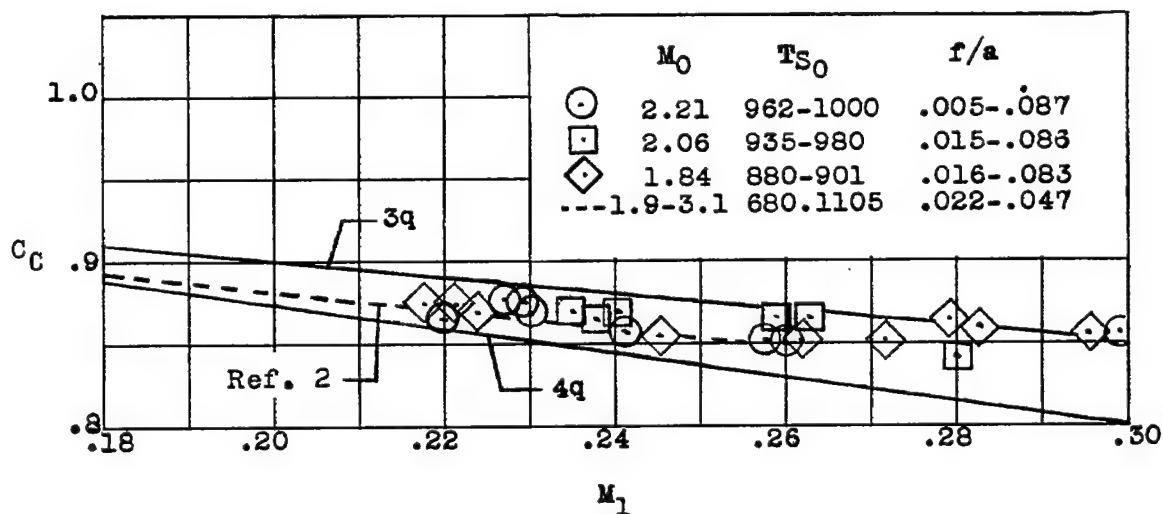
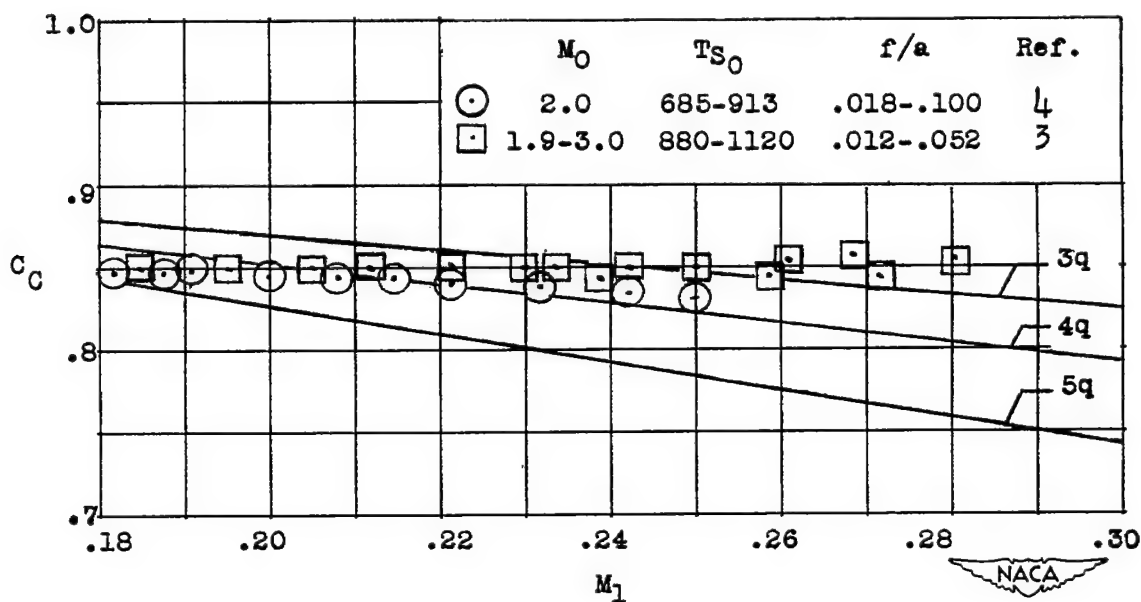


Figure 6.- Combustor B. Nonexpanding exit, $A_4/A_3 = 1.25$; double-row multiflameholder.



(a) $A_4/A_3 = 1.17$.



(b) $A_4/A_3 = 1.275$.

Figure 7.- Combustor C. Expanding exit, multiflameholder.

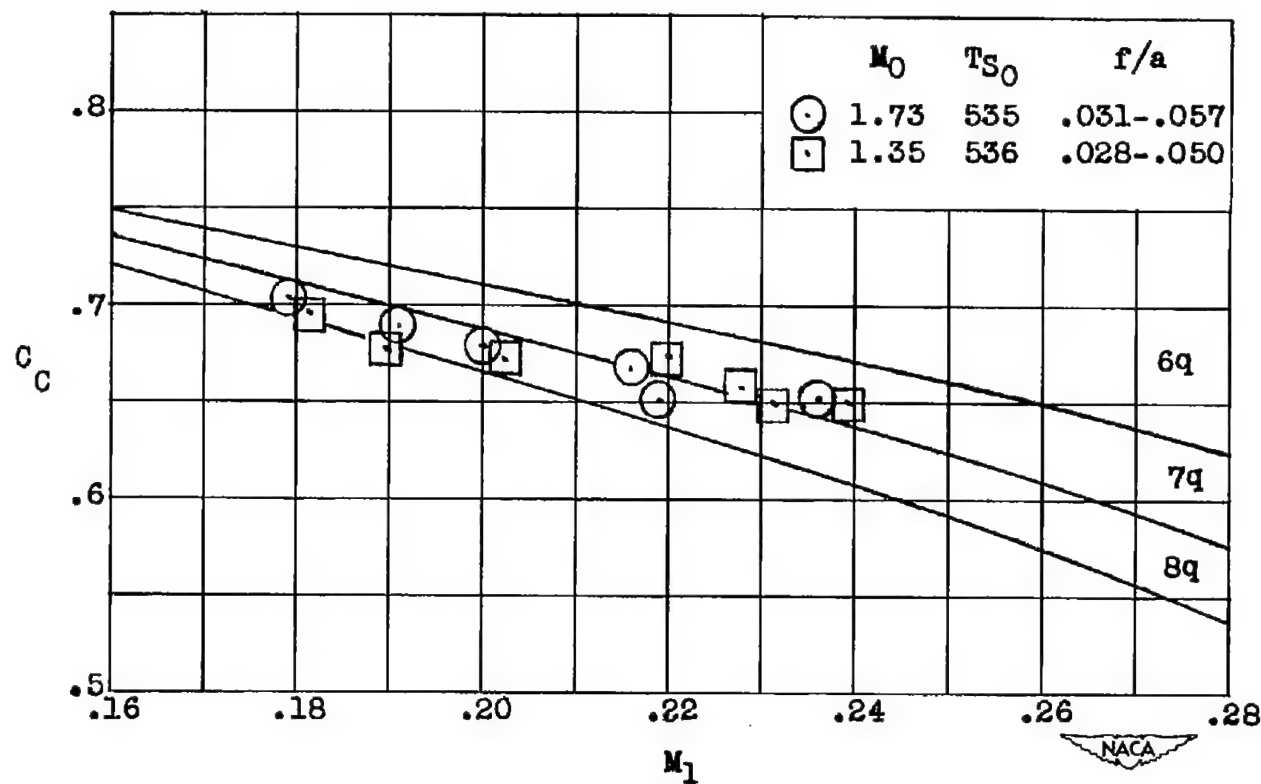
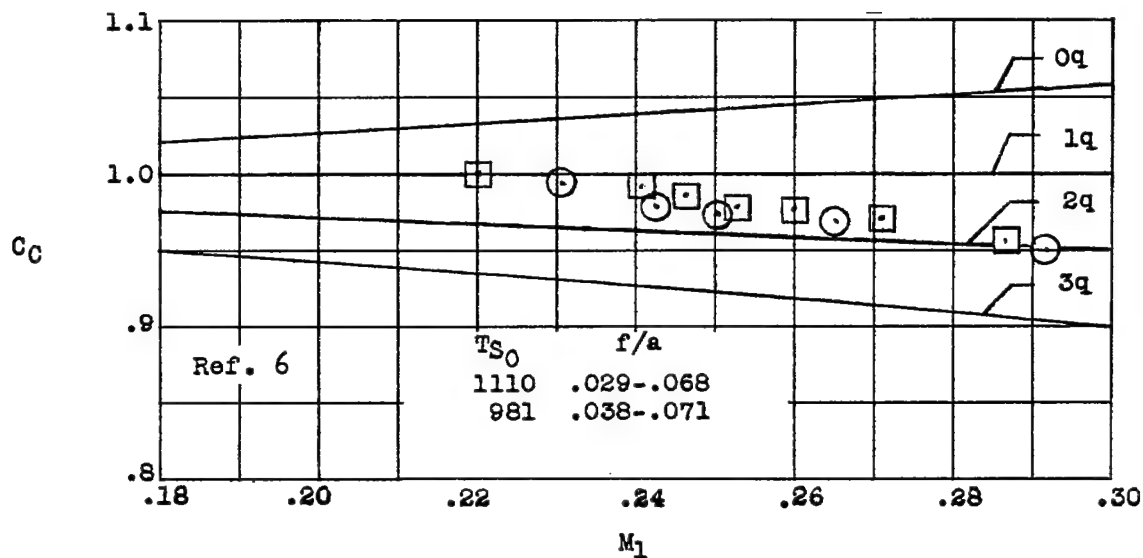


Figure 8.- Combustor D. Nonexpanding exit, $A_{14}/A_3 = 1.35$; corrugated-gutter flameholder. Data were obtained from reference 5.



(a) Straight pipe exit.

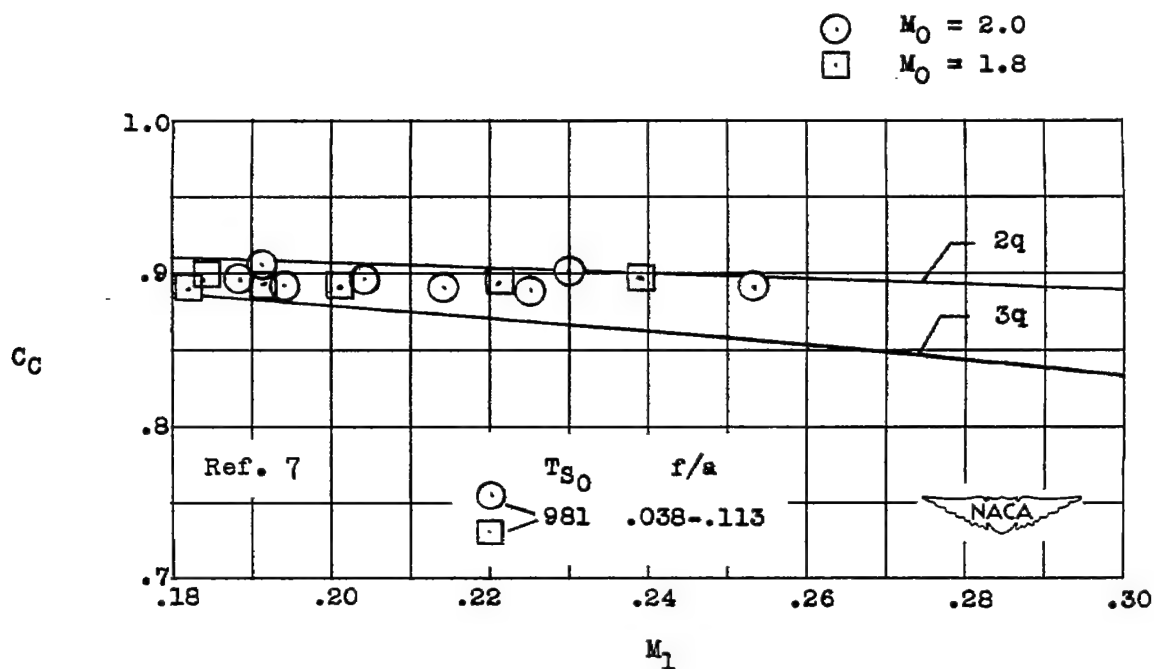
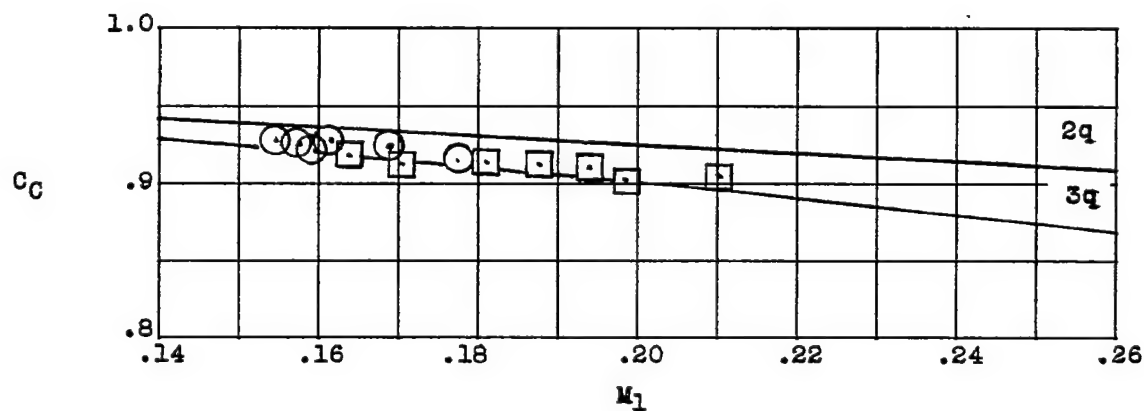
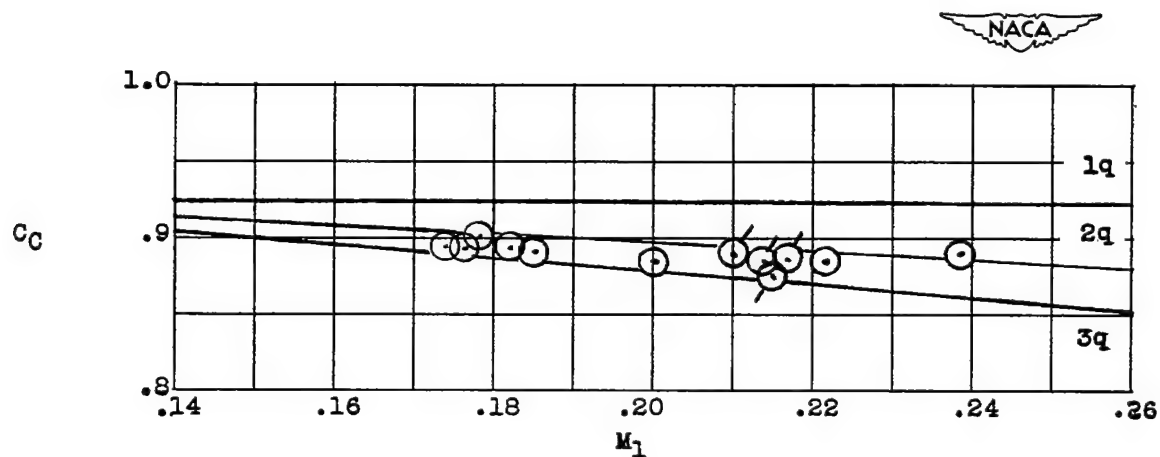
(b) $A_4/A_3 = 1.4$ (expanding exit).

Figure 9.- Combustor E showing effect of constant area and expanding exit on combustor coefficient. Data obtained from references 6 and 7.



(a) $A_4/A_3 = 1.17$.

Combustor type	M_0	T_{S0}	f/a
○ F	2.06	930	.034-.095
□ F	Connected duct	810	.045-.107
○ G	2.06	830	.025-.067



(b) $A_4/A_3 = 1.28$, expanding exit.

Figure 10.- Magnesium slurry combustors F and G.

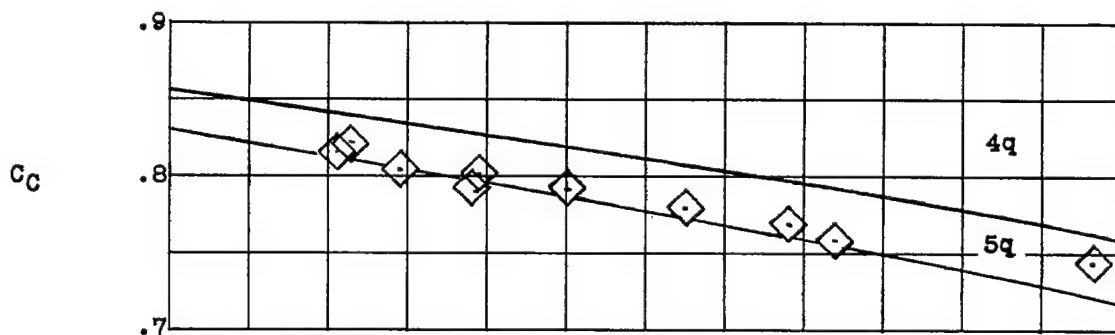
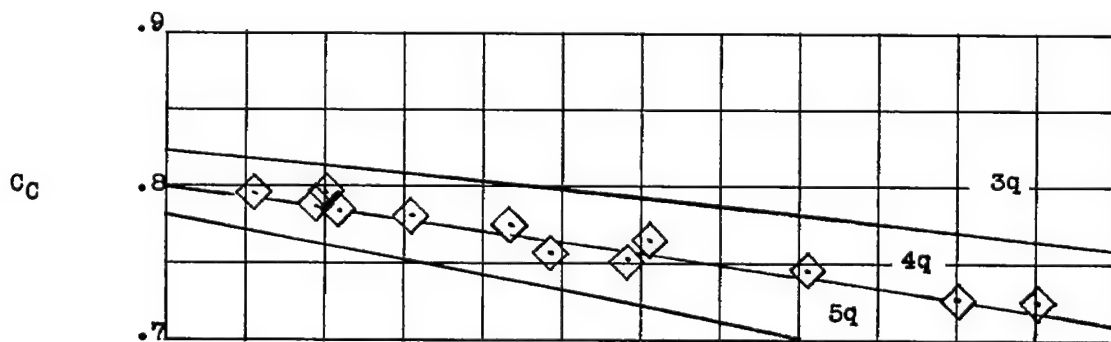
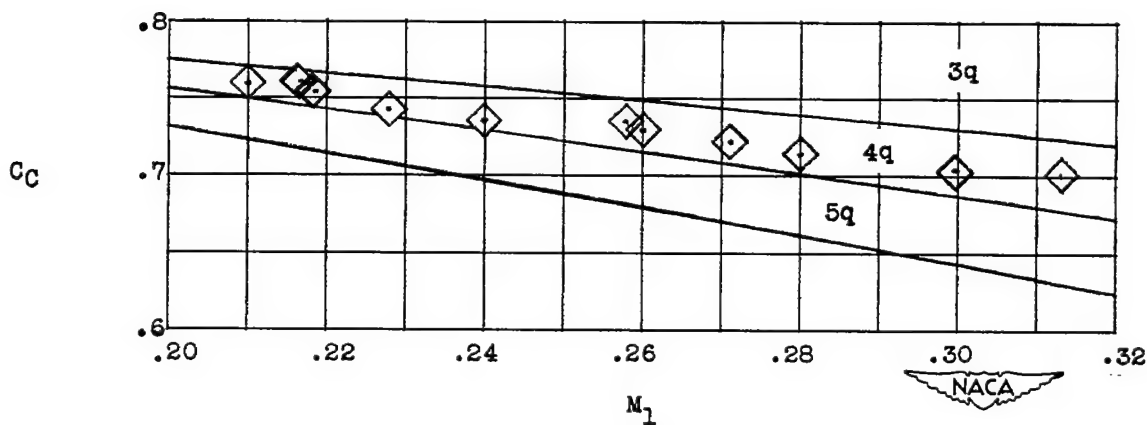
(a) $A_4/A_3 = 1.15$.(b) $A_4/A_3 = 1.25$.(c) $A_4/A_3 = 1.37$.

Figure 11.- Combustor A showing the effect of exit nozzle size on combustor force coefficient C_c for nonexpanding exit conditions at $M_0 = 1.84$.

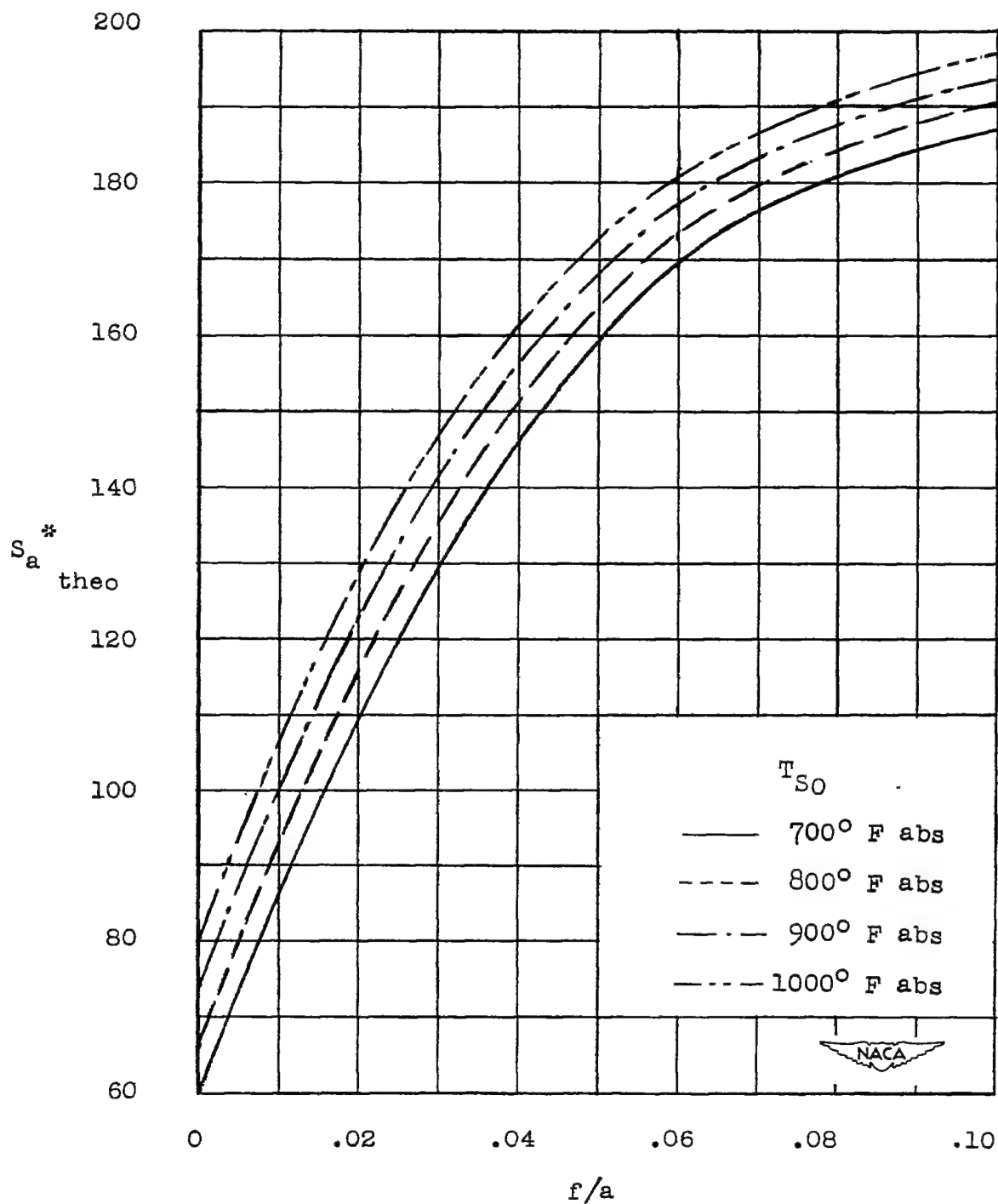


Figure 12.- Variation of theoretical air specific impulse S_a^* with fuel-air ratio at different T_{S0} for a typical hydrocarbon fuel.

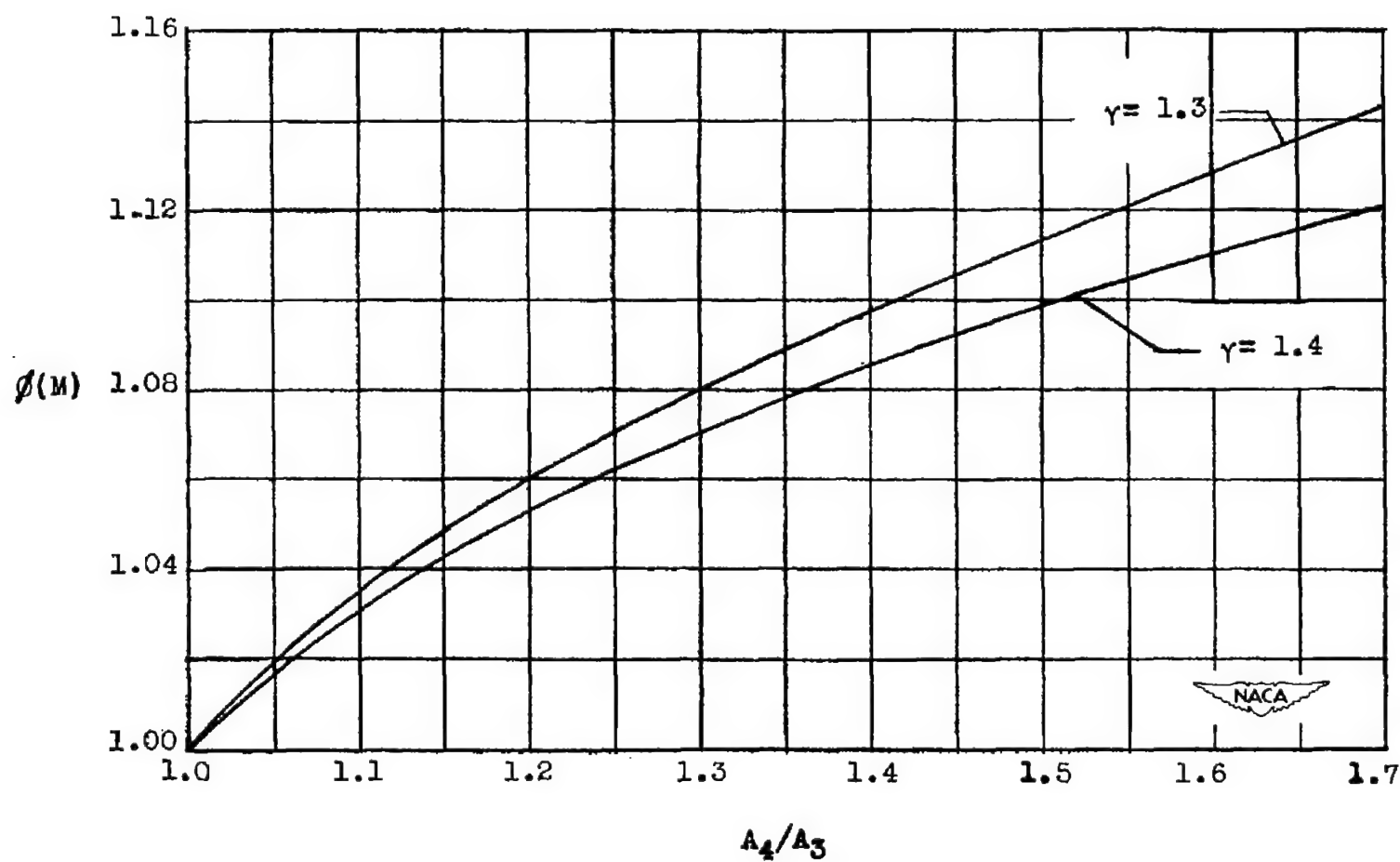


Figure 13.- Nozzle correction factor $\phi(M)$ against expanding area ratio.

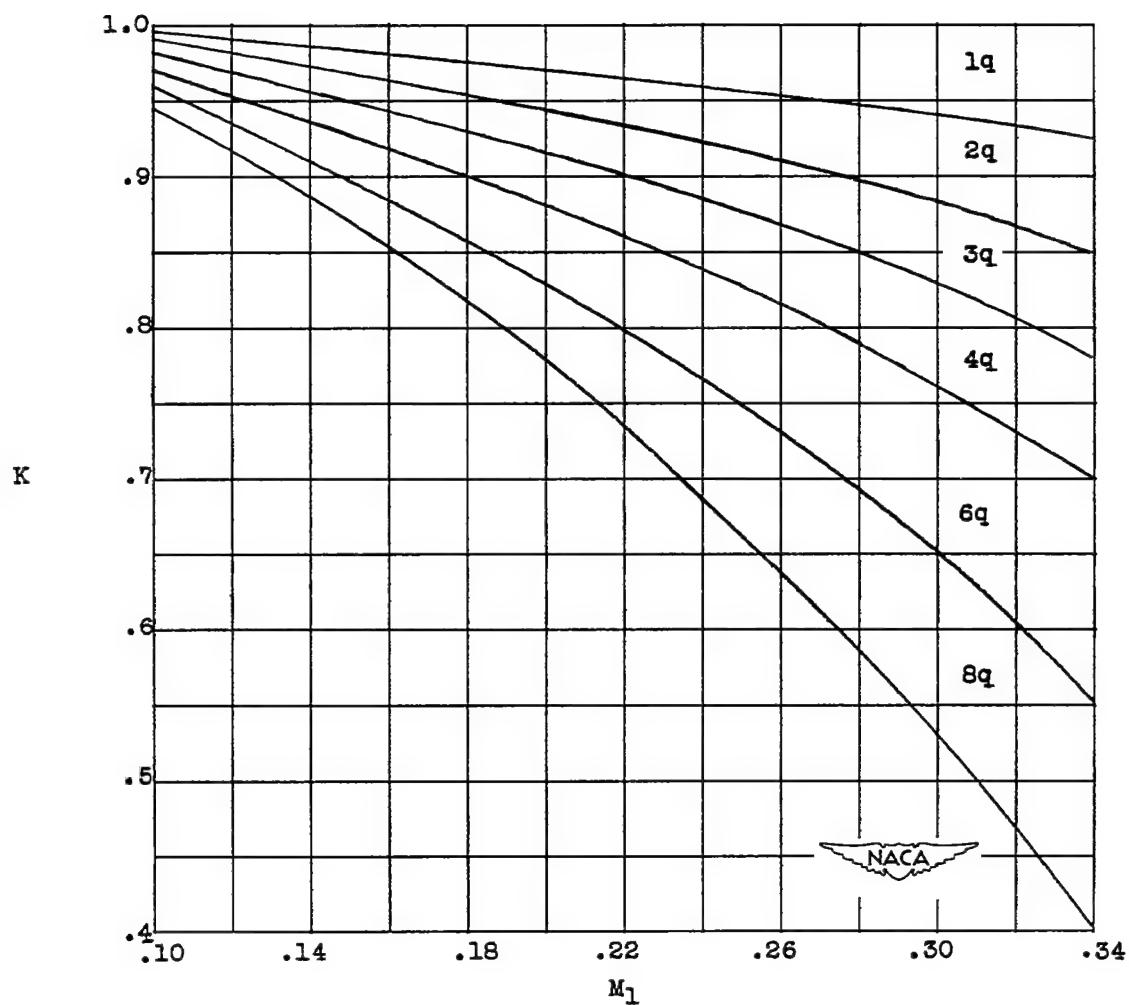


Figure 14.- Total-pressure ratio K against M_1 for various internal-drag conditions.

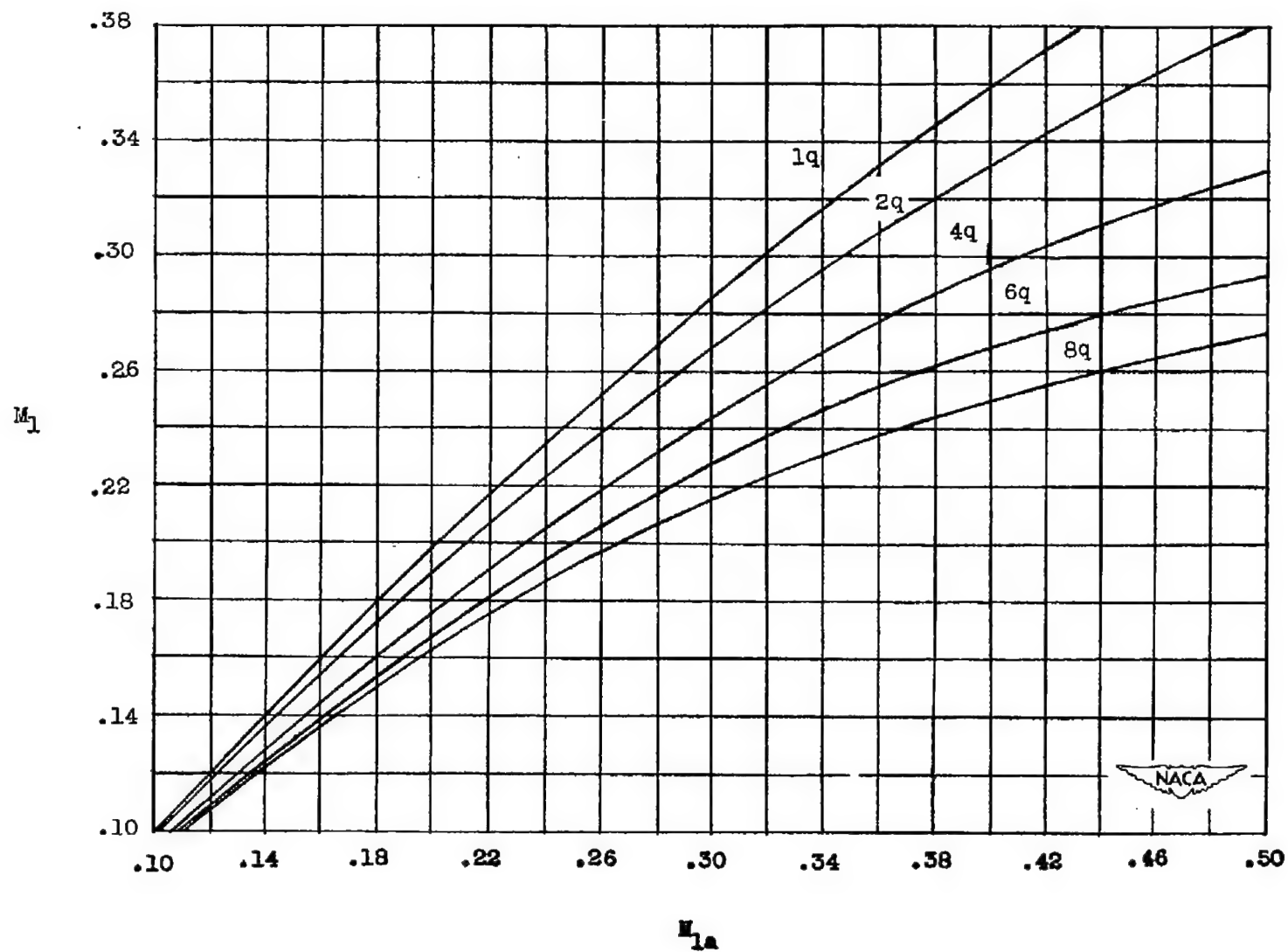
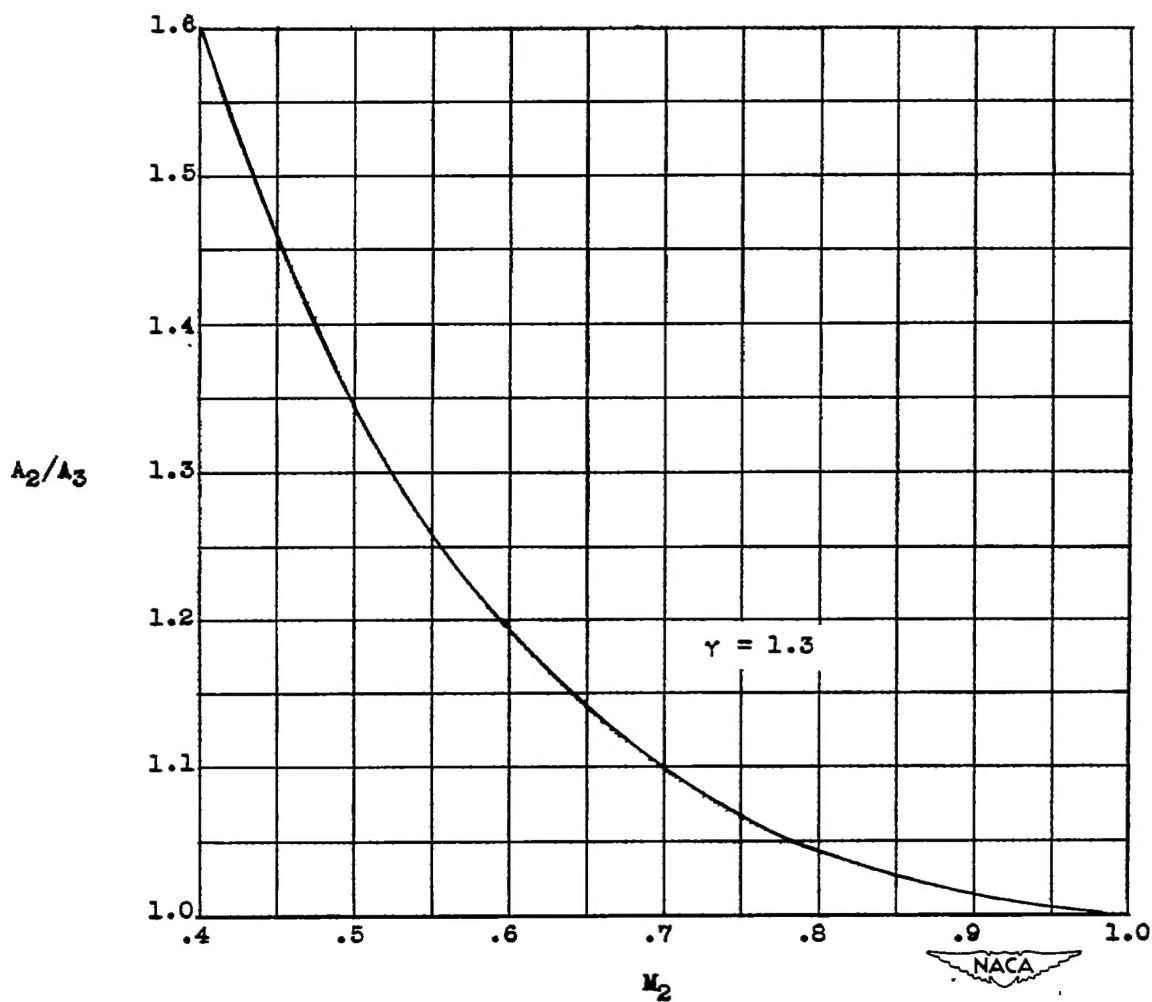
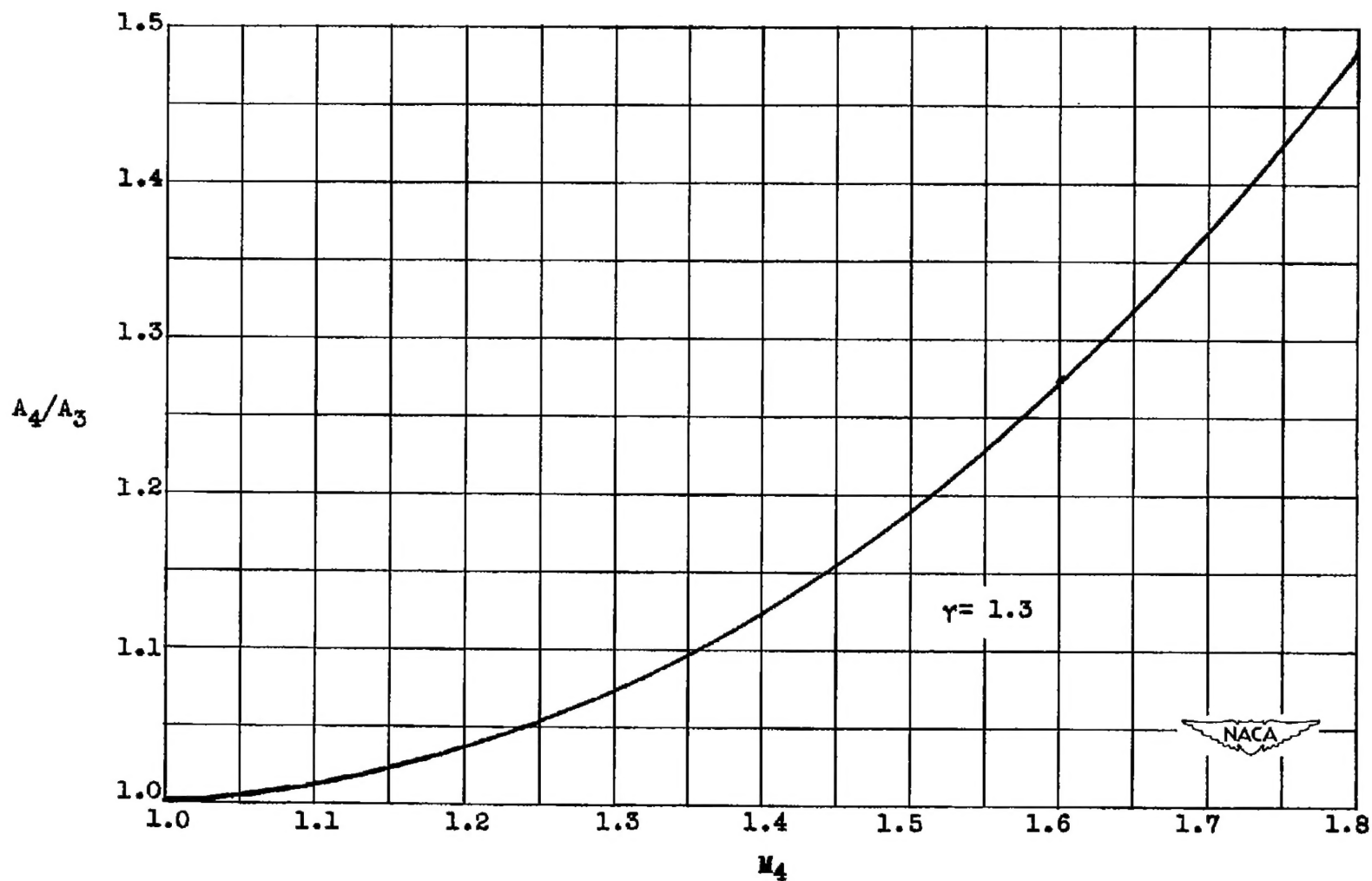


Figure 15.- Mach number change due to internal-drag losses in terms of q_1 .



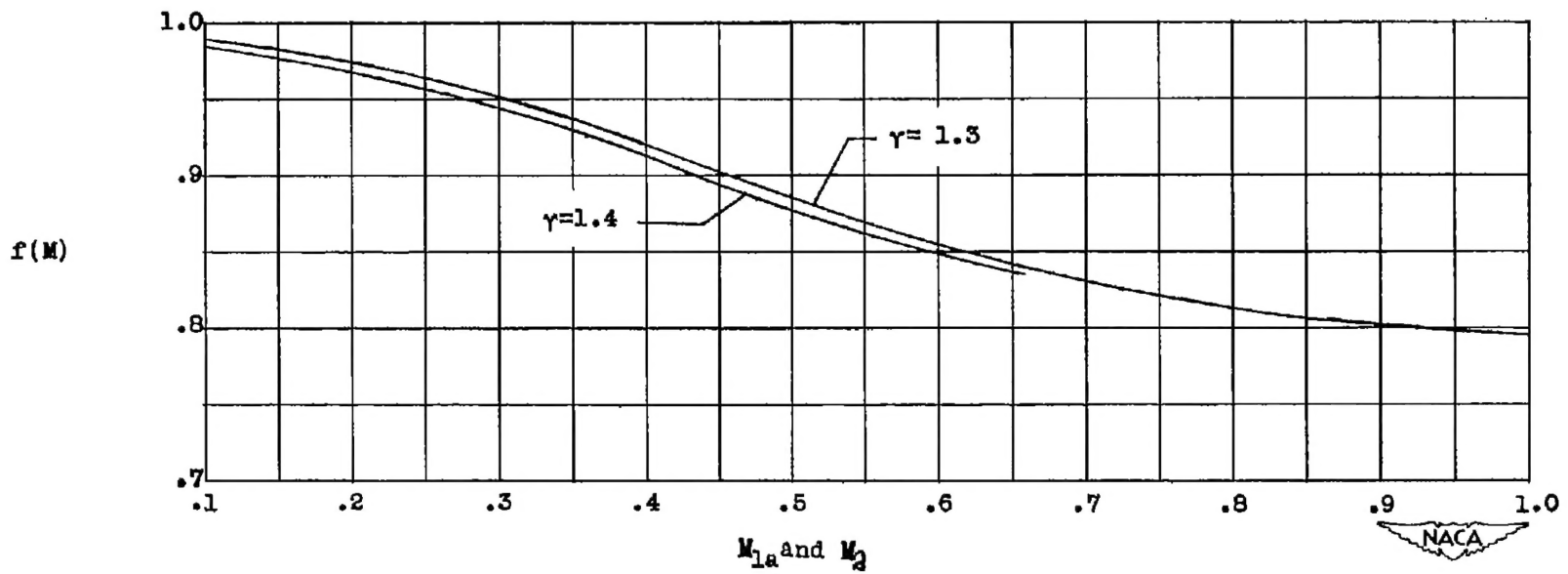
(a) Subsonic.

Figure 16.- Isentropic Mach number variation with exit-nozzle area ratio.



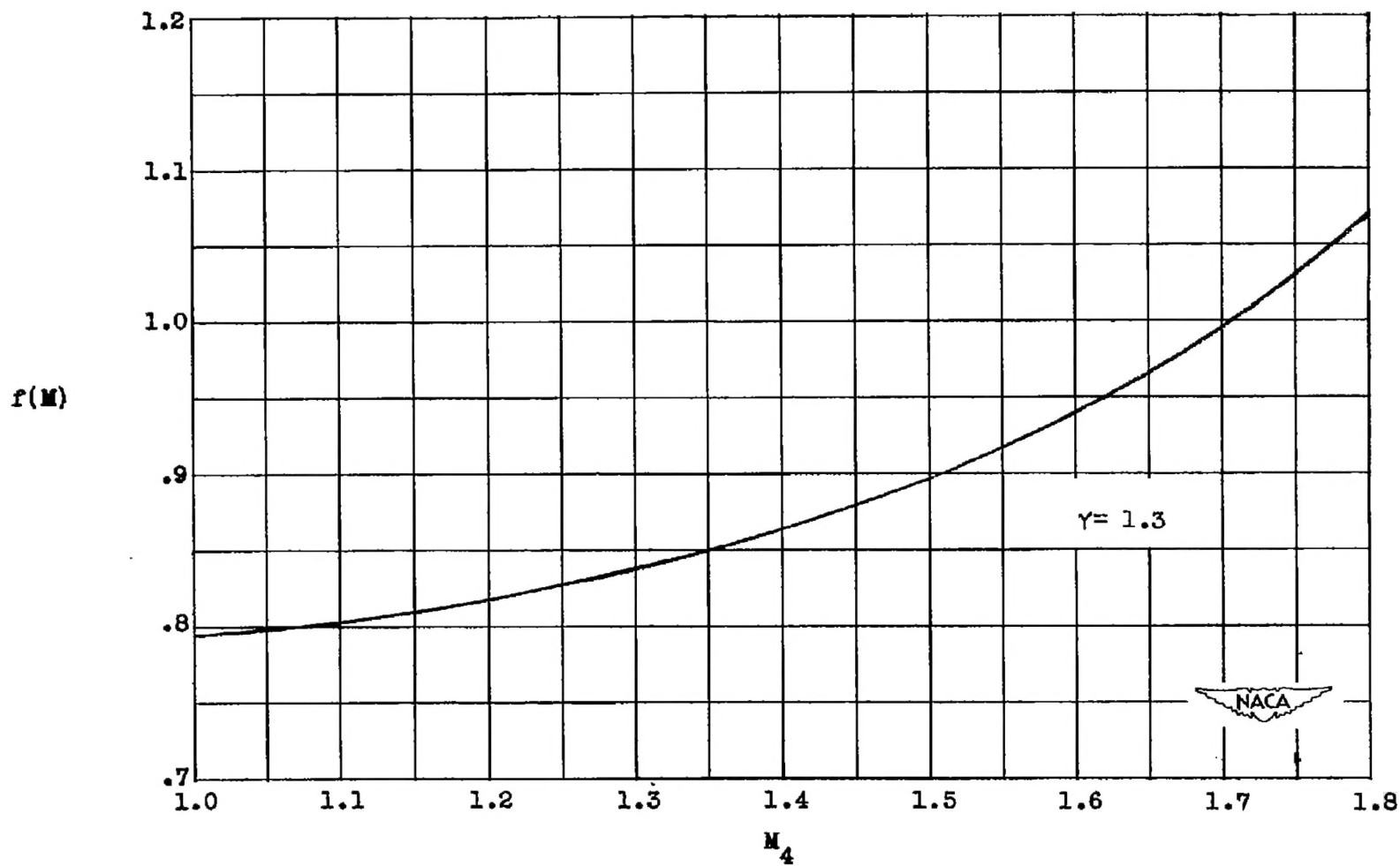
(b) Supersonic.

Figure 16.- Concluded.



(a) Subsonic.

Figure 17.- $f(M)$ plotted against M_{1a} and M_2 .



(b) Supersonic.

Figure 17.- Concluded.